LAWRENCE
LIVERMORE
NATIONAL
LABORATORY

LLNL-JRNL-850747

Storage and persistence of organic carbon in the upper most three meters of soil under arable and native prairie land use

C. O. Anuo, L. Li, K. C. Moreland, K. J. McFarlane, A. Malakar, J. A. Cooper, B. Maharjan, M. Kaiser

June 26, 2023

Plant and Soil

Disclaimer

Storage and persistence of organic carbon in the upper three meters of soil under arable and native prairie land use

Christopher O. Anuo [1]*, Lidong Li [1], Kimber C. Moreland [2], Karis J. McFarlane [2], Arindam Malakar [3], Jennifer A. Cooper [4], Bijesh Maharjan [1], Michael Kaiser [1]

[1]Department of Agronomy & Horticulture, University of Nebraska-Lincoln, 202 Keim Hall, Lincoln, NE 68583-0915, USA.

[2]Center for Accelerator Mass Spectrometry, Lawrence Livermore National Laboratory, 7000 East Ave, Livermore, CA, 94551, USA.

[3] Nebraska Water Center, part of the Robert B. Daugherty Water for Food Global Institute and School of Natural Resources, University of Nebraska, Lincoln, NE 68583-0844, USA.

[4]Nutrien, 4516 N Howard Avenue, Kerman, CA, 93630, USA.

Authors email addresses:
Christopher O. Anuo - canuo2@huskers.unl.edu: * Corresponding author
Lidong Li -lli32@unl.edu
Jennifer A. Cooper - jennifer.cooper@nutrien.com
Kimber C. Moreland - moreland3@llnl.gov
Karis J. McFarlane - kjmcfarlane@llnl.gov
Arindam Malakar - amalakar2@unl.edu
Bijesh Maharjan - bmaharjan@unl.edu
Michael Kaiser - mkaiser6@unl.edu

Abstract

Aims - Land use change from native grasslands to arable lands globally impacts soil ecosystem functions, including the storage of soil organic carbon (SOC). Understanding the factors affecting SOC changes in topsoil and subsoil due to land use is crucial for effective mitigation strategies. We determined SOC storage and persistence as affected by land use change from native prairies to arable lands.

Methods - We examined SOC stocks, soil $\delta^{13}C$ and $\Delta^{14}C$ signatures, microbial community (bacteria and fungi), and soil mineral characteristics under native prairies and long-term arable lands (i.e., > 40 years) down to 3 m in the U.S. Midwest.

Results - Native prairie soils had higher SOC stocks in the A horizon and 0-50 cm depth increment than arable soils. For both land use types, the $\delta^{13}C$ and $\Delta^{14}C$ values significantly decreased with depth, with the latter pointing towards highly stabilized SOC, especially in the B- and C-horizons. Analysis of microbial communities indicated that the diversity of bacteria and fungi decreased with soil depth. The content of oxalate soluble Al appeared to be the single most important predictor of SOC across horizons and land use types.

Conclusion - Our data suggest that most SOC gains and losses and transformation and translocation processes seem to be restricted to the uppermost 50 cm. Increasing SOC retention in A and B horizons within the 0-50 cm depth would enhance organic material serving as substrate and nutrients for microbes and plants (A horizon) and facilitate long-term SOC storage in subsoil (B horizon).

Keywords: Land use, C_4-C_3 vegetation, $\delta^{13}C$, and $\Delta^{14}C$, soil organic carbon persistence, Microbial communities.

Abbreviations: SOC, soil organic carbon; N_t, soil total nitrogen; M-DNA, microbial DNA.

Introduction

Essential ecosystem services largely affected by soil organic carbon (SOC) levels, such as nutrient supply, climate change mitigation, and water retention, are provided by both undisturbed and managed soils (Franzluebbers, 2021; Cotrufo and Lavallee, 2022). Soils store more carbon than the earth's atmosphere and living biomass combined, and about 50 to 70% of SOC is stored below 30 cm, highlighting the importance of subsoil for terrestrial carbon storage (Jobbagy and Jackson, 2000; Possinger et al., 2021; Moreland et al., 2021). However, uncertainty remains in our process-level understanding of how land use and soil management affect SOC storage, especially with depth (Yost and Hartemink, 2020). Furthermore, such uncertainty may affect estimations of carbon exchange rates between the soil and atmosphere as a response to changes in land use and soil management (Harrison et al., 2011; Gross and Harrison, 2019). Understanding drivers of subsoil SOC dynamics in different land use systems is critical for sustainable and climate-smart management strategies.

The intensification of land use has led to significant changes in SOC storage and turnover compared to undisturbed conditions under native vegetation (Ogle et al., 2005; Lal, 2019; Cotrufo and Lavallee, 2022). Over the course of human agricultural history, which began about 12,000 years ago, intensively managed arable soils have lost nearly 26% of their SOC stock in the top 30 cm and over 16% in the top 100 cm, resulting in a global estimated loss of about 116 Pg of carbon from the upper 2 m of soils (Sanderman et al., 2017). In the U.S. Great Plains, intensively managed arable soils, which produce approximately three-quarters of the country's corn and soybeans, have suffered some of the most significant losses. Here, up to 50% of SOC has been lost since agricultural expansion started in the 19th century (Malo et al., 2005; Paustian et al., 2019; Sanford et al., 2022). When scaled to arable land areas in the region, such intensified cultivation has led to

a loss of about 1100 Tg of carbon, particularly in the top 30 cm of soil (Liebig et al., 2009). These losses were mainly due to lower organic carbon (OC) input, destruction of soil aggregates, which reduces SOC stabilization, and soil erosion (Sanford et al., 2022). There is growing interest in managing agricultural soils as carbon sinks to reverse historical carbon losses and mitigate rising atmospheric carbon levels, emphasizing the need for detailed information on land use change impacts on SOC storage and persistence (Paustian et al., 2016; Sanderman et al., 2017).

Prerequisites for using the subsoil to store more OC in the long-term are systems that allow for increased OC translocation in this soil compartment. Increasing belowground deep root-derived carbon inputs has been suggested to foster long-term retention of OC in arable soils (Lal, 2019; Slessarev et al., 2020; Wang et al., 2022). The direct contact of root litter-derived carbon with protective soil minerals and the release of small, highly reactive root exudates and rhizodeposits, which may also stimulate microbially derived carbon inputs, can contribute significantly to SOC retention in the subsoil (Dijkstra et al., 2021; Bai and Cotrufo, 2022). Such strategies may include cultivating deep-rooted perennials and cover crops or converting arable soils to grassland (Rasse et al., 2005; Beniston et al., 2014; Cagnarini et al., 2019). In contrast, inputs (e.g., root exudates and rhizodeposits) derived from deep-rooting vegetation may also facilitate SOC loss by weakening or releasing organic compounds from protective mineral associations through priming (Keiluweit et al., 2015). Thus, the extent to which different biotic and abiotic factors control SOC accumulation and loss across depths remains largely unknown. The amount and turnover of SOC under native vegetation with minimal disturbance can serve as a benchmark for SOC accumulation in intensively used agricultural sites (Cotrufo and Lavallee, 2022). Such comparisons can be used to delineate soil environmental conditions under which the highest SOC gains or losses can be

expected in response to land use or management changes (Follett et al., 2012; Amelung et al., 2020; Maharjan et al., 2020).

Subsoils store most of the OC for centuries to millennia, making them ideal locations for long-term carbon storage, which has implications for climate change mitigation (Scheibe et al., 2023; Sierra et al., 2024). While subsoils generally have lower concentrations of SOC compared to topsoils, their larger volume results in greater SOC storage (Angst et al., 2018; Moreland et al., 2021). The larger potential for long-term carbon storage in the subsoil is further amplified by the predominance of SOC, which is more protected from microbial access and a subsoil environment that is less prone to disturbance than the topsoil (Rumpel and Kögel-Knabner, 2011; Hicks Pries et al., 2018; Wang et al., 2022). Understanding how land use change impacts subsoil is key to capturing how this terrestrial subsystem that stores most of the SOC for longer periods of time might respond. This also includes examining changes in the structure of microbial communities (e.g., bacteria and fungi), which are linked to modifications in SOC dynamics across depths (Fierer et al., 2013; Mackelprang et al., 2018).

Major factors that impact SOC accumulation and persistence across the soil profile include climate, vegetation, soil microorganisms and their access to substrate and nutrients, parent material, and soil mineral characteristics (Viscarra Rossel et al., 2019; Wiesmeier et al., 2019; Vormstein et al., 2020). Previous studies have suggested that SOC accumulation and persistence in mineral soils result from interactions between organic matter (OM) and Fe and Al oxides or oxyhydroxides (Kleber et al., 2015; Hall and Thompson, 2021; Shimada et al., 2022). Other studies pointed toward the relevance of associations between OM and mineral surfaces via exchangeable cations (Nitzsche et al., 2017; Rasmussen et al., 2018; Rowley et al., 2018). Thus, variation in soil mineralogical characteristics dictated by soil parent material or soil type in different land use

157 systems will affect the magnitude of SOC retention across depths. Furthermore, the transformation
158 of plant material into microbially processed OM and retention of microbially derived biomass
159 (e.g., cell walls) have been discussed as critical processes within SOC stabilization and retention
160 in mineral soils (Cotrufo et al., 2013; Kallenbach et al., 2016), thus affecting SOC accumulation
161 and turnover. However, the impact of land use change on SOC stabilization processes and
162 mechanisms across soil depths or horizons and their biotic and abiotic driving factors remain
163 largely unclear. This is further exacerbated by the high variability in physical and chemical subsoil
164 properties and SOC origin across scales (Chabbi et al., 2009; Heckman et al., 2021; Nave et al.,
165 2021).

166 In this study, we aimed (1) to quantify soil depth-specific differences in SOC stocks in the
167 uppermost three meters of native prairie soils and arable soils, (2) to clarify the impact of soil
168 mineral characteristics on land use-specific SOC characteristics across soil horizons, (3) to
169 examine $\Delta^{14}C$ and $\delta^{13}C$ isotopic signatures of SOC to understand land use impact on carbon
170 stabilization and transformation, inputs, and losses across horizons, and (4) to evaluate the impact
171 of land use on soil microbial community structure across horizons. To address these objectives,
172 we sampled 11 native prairie sites and 11 arable sites in the US Midwest (Nebraska) and quantified
173 SOC stocks across soil horizons and depth increments. To identify factors and processes that
174 control SOC retention across soil horizons in both land use systems, we analyzed relationships
175 between SOC, soil characteristics (i.e., texture, soil pH, exchangeable Ca, and Mg, reactive Fe,
176 and Al phases), soil carbon isotope signatures ($\delta^{13}C$ and $\Delta^{14}C$), and microbial DNA concentration.
177 Based on differences in SOC characteristics between arable and native prairie sites, soil
178 environmental conditions were set out to be identified that might be most relevant for gains in
179 SOC within climate-smart management strategies.

Materials and Methods

Site description

We selected 11 native prairie sites and 11 arable sites whose soils predominantly developed from the parent material loess across Nebraska, as shown in Figure 1. The selected sites (listed in Table S1; USDA-NRCS, 2022) were picked from the major land resource areas (MLRAs) of the United States and were chosen to encompass a variety of soil characteristics and climatic variables. The native prairie sites are presumed to reflect the original state of the arable sites before they were cultivated. The general soil, climatic, and vegetation characteristics for all sites are summarized in Table S1. The native prairie soils and arable soils were moderately to well-drained, spanning a soil texture gradient. More than 80% of the vegetation cover in the native prairie sites consists of a mixture of short, mid, and tall C_3 and C_4 grasses. The arable sites were long-term (> 40 years) continuously cropped fields, mainly under corn (*Zea mays, L.*) and soybean (*Glycine max*) rotations. The most common management practices adopted in the arable sites include cover cropping, no-till or reduced-till, fertilizer application, and irrigation (Table S1).

Soil sampling and processing

Samples were collected from each native prairie and arable site between November 2020 and May 2021. In each site, soil was collected from a uniform flat area, free of signs of erosion caused by wind or water. Soil cores were collected from three random locations per site (~ 1 m apart), representing three pseudo-field replicates as continuous cores from 0-50, 50-100, 100-200, and 200-300 cm depth increments (i.e., 300 cm) using a Genuine Geoprobe (3.45 cm core diameter, Geoprobe systems, Salina, KS). After sampling, soil cores were wrapped in aluminum foil, stored in cool containers (with ice packs), transported to the laboratory, and frozen at -80°C until

processed. The frozen cores were unpacked during processing, and the entire 300 cm soil core was split according to the major pedogenetic horizons (A, B, and C). Samples for microbial analysis were collected from each horizon and immediately stored at -80 ℃. The remaining bulk soil samples from each horizon of the three random soil cores per site were air-dried, sieved to pass through a 2 mm sieve, and stored in glass jars.

Bulk soil physical-chemical characteristics

All laboratory measurements were performed on air-dried soils except soil used for microbial analysis and bulk density determination. Moisture corrections were done by calculating the mass difference between air-dried soils and soils oven-dried overnight at 105℃ (Wood and Bowman, 2021). Bulk density was determined using the intact soil core method (both fine and coarse particles), as described by Grossman and Reinsch (2002), and soil pH (1:1 water) was measured following the procedure described by Miller and Kissel (2010). Particle size distribution: sand (50-2000 μm), silt (50-2 μm), and clay (<2 μm) was determined using the hydrometer method (Gee and Or, 2002). Macronutrient analyses were performed to determine available N-NO_3 using the KCl extraction method (Doane and Horwάth, 2003), available S-SO_4, and P-PO_4^3 using the Mehlich 3 extraction method (Schulte and Eik, 1988; Mallarino, 2003; Pittman et al., 2005). Exchangeable base cations (Ca, K, and Mg) were determined by the ammonium (NH_4^+) acetate (AA) extraction method. Reactive Fe and Al phases were determined by acid ammonium (NH_4^+) oxalate (AO) (targeting short-range ordered phases and organo-metal complexes) and dithionite-citrate bicarbonate (DCB) (targeting highly crystalline oxides as well as short-range ordered phases) extraction methods following the standard USDA-NRCS procedure (Soil Survey Staff, 2014). Briefly, for AO extraction, Tamm reagent (acid ammonium oxalate, 0.2 M, pH 3) was

prepared by dissolving 16.15 g of ammonium oxalate and 10.90 g of oxalic acid in 1 L of Milli-Q water (resistivity of 18.2 MΩ). 1 g of air-dried soil (dried for 24 hours) was added to a 50 ml centrifuge tube, followed by 50 ml of the acid oxalate reagent. The mixture was gently shaken to mix and then equilibrated in darkness on a reciprocating shaker for 4 hours. After equilibration, the mixture was centrifuged for 5 minutes, and the extraction was collected and analyzed for Fe and Al in inductively coupled plasma mass spectroscopy (Thermo Dionex IC 5000+ iCAP RQ ICP MS). For DCB extraction, 79.4 g of trisodium citrate and 9.24 g of sodium bicarbonate were dissolved in 1 L of Milli-Q water, resulting in a buffer solution with a pH of approximately 7.3. In a 50 mL centrifuge tube, 3 g of air-dried soil sample was added and mixed with 45 mL of the buffer solution. The mixture was agitated in a hot water bath at 75 °C for 15 minutes. Then, 1 g of sodium dithionite was added, and the mixture was kept in the hot water bath for an additional 10 minutes. Another 1 g of dithionite was then added very slowly, and the mixture was agitated in the water bath for another 15 minutes. Finally, the solution was cooled and centrifuged, and the supernatant was collected and analyzed for DCB-extractable Fe and Al using ICP-MS.

Soil organic carbon and total nitrogen

After ball-milling (SPEX SamplePrep, 8000D Mixer/Mill) the soil samples, total soil carbon and nitrogen (N_t) in percent (%) were measured by dry combustion using an elemental analyzer (Thermos Scientific, Waltham, MA, USA). Before the analysis, an effervescence test conducted by application of 10% HCl was used to determine if any inorganic carbon was present. When carbonates were detected, soil inorganic carbon content was quantified using the modified pressure calcimeter method (Digital Gauge Model Kit+Mixer, HMLS) described by Sherrod et al. (2002). The soil inorganic carbon content was subtracted from the total carbon to obtain the SOC content.

The SOC stocks (kg m^{-2}) were calculated for each identified horizon according to their respective depths, although some cores had more than one B and C horizon. If, for example, two B horizons were identified (i.e., B_1 and B_2), the stocks from each horizon were summed to calculate the total stock for the B horizon ($B = B_1 + B_2$). For the fixed depth increments, SOC stocks were summed to obtain the cumulative SOC stocks for the 0-50, 50-100, 100-200, and 200-300 cm depth increments, considering the specific contribution of individual pedogenic horizons to each increment. Across horizons, bulk density between arable and native prairie soils was not different (Table 1). Thus, an equivalent soil mass (ESM) approach was not applicable (Ellert et al., 2002; Wendt and Hauser, 2013).

*SOC stocks (kg m^{-2}) =SOC concentration (g kg^{-1}) * [Bulk density (g cm^{-3}) * Volume (cm^3)] (Eq. 1). Where volume is the product of area (cm^2) multiplied by depth (cm).*

Bulk soil samples from A, B, and C horizons were analyzed for $\delta^{13}C$ and for $\Delta^{14}C$. Specifically, selected samples from these horizons across land use types were utilized for $\Delta^{14}C$ analysis. Samples that contained carbonates were initially treated following the acid fumigation method, as described by Harris et al. (2001). However, this method did not completely eliminate the carbonates in several samples. Samples that showed effervescence and a $\delta^{13}C$ less negative than -12‰ after fumigation were treated with the acid soaking and drying method described by Slessarev et al. (2020) to ensure complete removal of the carbonates. For $\delta^{13}C$ analysis, samples were measured using the Thermo Finnigan Delta Plus isotope-ratio mass spectrometer (IRMS) interfaced with a Carlo Erba Elemental Analyzer (Thermo Finnigan, San Jose, CA). For $\Delta^{14}C$ analysis, analyzed as graphite using the NEC 1.0 MV Model 3SDH-1 or FN van de Graff tandem accelerator mass spectrometer at the Center for Accelerator Mass Spectrometry (Lawrence

Livermore National Laboratory, Livermore, CA, USA) following the method of Broek et al. (2021). Briefly, soil samples were weighed into quartz tubes containing cupric oxide and silver under a vacuum. After the tubes were sealed, the samples were converted to CO_2 by heating at 900 °C for 6 hours. In the presence of hydrogen gas and Fe catalyst, the CO_2 was reduced to graphite at 570 °C (Vogel et al. 1987). Data were corrected for mass-dependent fractionation using the measured $\delta^{13}C$ values (i.e., differential partitioning of carbon isotopes based on their masses) and are reported in $\Delta^{14}C$ notation corrected for the year of measurement (2022) and conventional radiocarbon age (based on the Libby half-life) following Stuiver and Polach (1977). Conventional radiocarbon ages are provided for reference and should not be interpreted as actual ages, as soils are open systems with respect to OC.

Soil microbial community analyses

To determine the diversity and composition of microbial communities (bacteria and fungi), soil DNA was extracted from 0.25 g subsamples of each horizon from two cores of 10 sites (i.e., pseudo field replicates) using the DNeasy PowerSoil Pro Kits (QIAGEN, Hilden, Germany). The concentrations of purified DNA were verified using a spectrophotometer (NanoDrop, ND2000, Thermo Scientific, USA). Amplification and sequencing of DNA were performed at the Argonne National Laboratory in Lemont, IL, using Illumina MiSeq (Illumina Inc., San Diego, CA, USA). The bacterial V4 hypervariable regions of the 16S rRNA gene and fungal internal transcribed spacer (ITS) region were amplified using the primer pair 505F/816R (Caporaso et al., 2011, 2012) and ITS1F/ITS2 (Buée et al., 2009), respectively. The raw DNA sequence data were analyzed using QIIME2-2021.11 (Bolyen et al., 2019). The *q2-dada2* plugin was used for sequence quality control and feature table construction (Callahan et al., 2016). Sequences were trimmed to remove

low-quality regions, and trimming parameters were determined according to the quality plots. The phylogenetic tree was generated using the *align-to-tree-mafft-fasttree* pipeline from the *q2-phylogeny* plugin (Katoh et al., 2002). Sequences were rarefied for downstream analyses to ensure comparability across samples. Rarefaction depth was chosen to retain more sequences per sample while excluding as few samples as possible on the condition that the richness in the samples is fully saturated. The alpha diversity was analyzed with the *q2-diversity* plugin.

Statistical analysis

A two-way mixed model ANOVA was used to determine the main and interaction effect of land use and soil depths or horizons on soil biogeochemical characteristics (Glimmix procedure; SAS 9.4, SAS Institute Inc., Cary, NC, USA). Since pedon-scale SOC storage is often controlled by horizon thickness (i.e., vertical depth of each distinct layer), analysis of patterns by both horizon and fixed depth approaches is crucial for understanding genetic soil formation processes that are relevant to OC accumulation and persistence within the soil profile (Li et al., 2023). Land use was treated as a fixed factor, with depths or horizons as repeated measure variables and block (site) and replications as random variables. Means were compared using Fisher's Least Significant Difference. Data were log-transformed to achieve normal distribution when necessary. The univariate procedure was used to check for the normality of residuals, and Shapiro-Wilk's test was used to determine normality. Levene's test was used to assess the equality of variance. Results were reported as untransformed mean ± standard error. Pearson correlation was used to evaluate the relationships between SOC and N_t concentrations, soil mineral characteristics, soil carbon isotope signatures, soil microbial DNA concentrations, and soil nutrients. Correlations were performed separately by horizon (A, B, and C) and land use type (native prairie and arable). If

318 more than one horizon was detected for one of the three major horizons, e.g., B_1 and B_2, or C_1 and
319 C_2, the respective results were treated as individual data points in the correlation analyses. We also
320 used results from each core per site (three pseudo-field replicates) as individual data points. Data
321 were normally distributed and linear with no outliers. Significance was set at $p \leq 0.05$. The errors
322 reported in the text and tables are standard errors.

323 Further, we used structural equation modeling (SEM) (*semopy*; Python 3.12) to measure the
324 impact of management intensity and soil horizon on SOC and other soil properties and illustrate
325 how these variables interact with each other to produce the overall effect. We followed the
326 procedures for developing a structural equation model outlined by Li et al. (2019). We initially
327 proposed a hypothesized model according to background information and then tested the
328 significance of these pathways. The path coefficients were tested by maximum likelihood
329 estimation at $p \leq 0.05$. We reported the standardized path coefficients that are based on standard
330 deviation units. Data were scaled using *StandardScaler* from *scikit-learn*. Model fit was evaluated
331 by the goodness of fit index (GFI) and the comparative fit index CFI.

332

333 **Results**

334 *Chemical and physical bulk soil characteristics*

335 For sites under arable and native prairie land use, soil characteristics such as pH, bulk density,
336 texture, exchangeable base cations, and reactive Fe and Al oxides observed in A, B, and C horizons
337 are presented in Tables 1 to 3. Table 1 also includes information regarding the depths of the
338 individual soil horizons, highlighting the upper and lower depth ranges. Across different sites and
339 soil depths (i.e., from A to C horizon), soil pH measured in water ranged from 5.3-8.8 for arable
340 soils and 5.6-8.6 for native prairie soils (Table 1). Silt and clay contents in arable soils ranged from

8.0-74% and 1.3-38%, respectively, whereas in native prairie soils, they ranged from 0-72% and 2.0-34% (Table 1). For reactive Fe and Al oxides phases, we detected ammonium oxalate (AO) extractable Fe (Fe_{AO}) and Al (Al_{AO}) in the range of 42-2711 mg kg^{-1} and 178-1093, respectively, in arable soils, while in native prairie soils, they were found in the range of 35-2996 mg kg^{-1} and 34-1296 mg kg^{-1} (Table 3). Averaged across all sites within each land use system, $N\text{-}NO_3$ and $P\text{-}PO_4$ were significantly higher in arable soils than in native prairie soils in the A horizon. Nitrate-N was also significantly higher in the C horizon of arable soils than in native prairie soils (Table S2).

Contents and stocks of bulk soil organic carbon and total nitrogen across soil profiles

Across all 11 sites under arable and native prairie land use, the SOC and total nitrogen (N_t) contents in the A horizon ranged from 5.5-22 g kg^{-1} (SOC) and 0.5-1.8 g kg^{-1} (N_t) in arable soils and from 7.0-36 g kg^{-1} (SOC) and 0.6-3.4 g kg^{-1} (N_t) in native prairie soils (Table 1). Land use significantly affected the average SOC and N_t in the A horizon, with larger contents observed in native prairie soils (22 ± 1.2 g kg^{-1} SOC, 1.9 ± 0.1 g kg^{-1} N_t) compared to soils under arable land use (13 ± 0.8 g kg^{-1} SOC, 1.2 ± 0.1 g kg^{-1} N_t). In the B and C horizons, SOC and N_t contents did not significantly differ between arable and native prairie soils.

The SOC and N stocks observed in the A, B, and C horizons are shown in Figure 2a and b. In the A horizon, the SOC and N_t stocks observed in arable soils ranged from 2.2-12 kg m^{-2} and 0.2-1.0 kg m^{-2}, respectively, compared to 3.2-13 kg m^{-2} (SOC) and 0.3-1.4 kg m^{-2} (N_t) found in the native prairie soils. Land use significantly affected SOC and N_t stocks only in the A horizon, with greater SOC and N_t stocks found in the native prairie soils (8.0 ± 0.9 kg m^{-2} SOC, 0.7 ± 0.1 kg m^{-2} N_t) compared to the arable soils (5.3 ± 1.0 kg m^{-2} SOC, 0.5 ± 0.1 kg m^{-2} N_t).

Considering fixed depth increments (Figure 3a and b), the stocks in 0-50 cm range from 2.7-11 kg m^{-2} SOC and 0.3-0.9 kg m^{-2} N_t in the arable soils and from 4.0-17 kg m^{-2} SOC and 0.4-1.4 kg m^{-2} N_t in the native prairie soils. Significant differences in SOC and N_t stocks were observed only in 0-50 cm depth but not for the 50-100 cm, 100-200 cm, and 200-300 cm depth increments. In 0-50 cm, the SOC and N_t stocks were greater in the native prairie soils (9.9 ± 0.9 kg m^{-2} SOC, 0.9 ± 0.1 kg m^{-2} N_t) compared to arable soils (7.0 ± 0.9 kg m^{-2} SOC, 0.6 ± 0.1 kg m^{-2} N_t). In the entire 300 cm depth profile, the total amount of SOC and N_t stocks ranged from 5.9-35 kg m^{-2} SOC and 0.6-3.1 kg m^{-2} N_t in arable soils compared to 6.0-35 kg m^{-2} SOC and 0.9-3.5 kg m^{-2} N_t in native prairie soils. Land use-derived differences in SOC and N_t for the total 0-300 cm were observed for paired sites where soils under arable and native prairie land use were directly adjacent (Pearl harbor, Wildcat, and Pokorny) (Table S3 and Table S4).

Horizon-specific bulk soil C/N ratio, $\delta^{13}C$ and $\Delta^{14}C$ signatures

The average C/N ratio of bulk soil in arable and native prairie soils was generally low across the A to C horizons (Figure S1). In arable soils, the C/N ratio ranged from 9.6-11, while in native prairie soils, it ranged from 9.0-14. However, no significant differences were observed between the land use systems for the individual horizons.

The bulk soil $\delta^{13}C$ values detected for the A, B, and C horizons significantly decreased with depth (i.e., from A to C horizons) independent from the land use type, as shown in Figure 2c and Table 4. Differences between land use types for specific pedogenetic horizons were not significant ($p > 0.05$). In the A horizon, an average $\delta^{13}C$ value of -15.8 ± 0.3‰ was observed for arable soils compared to -16.2 ± 0.2‰ found for native prairie soils. In the B horizon, -17.9 ± 0.5‰ was found for arable soils compared to -17.3 ± 0.5‰ detected for native prairie soils. In the C horizon, arable

soils show an average $\delta^{13}C$ value of -21.4 ± 0.4‰ compared to -22.3 ± 0.4‰ found for native prairie soils.

The bulk soil $\Delta^{14}C$ values for selected A, B, and C horizons significantly decreased with depth (i.e., from A to C horizons), which was observed for both land use systems (Figure 2d; Table 4). The average values for specific horizons indicated that land use significantly affected the $\Delta^{14}C$ value in the A horizon, with lower $\Delta^{14}C$ for arable soils (-118 ± 26‰) (i.e., more depleted) compared to native prairie soils (-7 ± 8.0‰) (i.e., less depleted). In the B horizon, significant differences in $\Delta^{14}C$ were not observed between arable (-518 ±75‰) and native prairie soils (-380 ± 83‰). Similarly, in the C horizon, significant differences were not detected between arable (-746 ± 33‰) and native prairie soils (-730 ± 38‰) ($p = 0.76$).

Horizon-specific bulk soil microbial DNA concentrations and microbial community structure

The average soil microbial DNA concentration observed for the individual horizons in arable and native prairie sites (i.e., 10 sites) decreased with depth, as shown in Figure 4a. In the A horizon, significantly larger microbial DNA concentrations (153.8 ±18 mg kg^{-1} soil) were observed in the native prairie soils compared to the arable soils (57.7 ±7.0 mg kg^{-1} soil). In the B horizon, the amount detected in the arable soils (12.6 ± 2.7 mg kg^{-1} soil) did not differ significantly from the amount observed in the native prairie soils (19.8 ± 5.0 mg kg^{-1} soil). A similar observation was made in the C horizon with no significant differences between the arable (7.5 ± 1.2 mg kg^{-1} soil) and native prairie soils (6.2 ±1.2 mg kg^{-1} soil).

Analysis of microbial communities showed that the diversity of bacteria and fungi decreased with depth and responded differently to the type of land use for the individual horizons (Figure 4b-e). In the A horizon, land use did not significantly affect the bacteria Faith's phylogenetic diversity

(Figure 4b) but influenced the distribution of species (Pielou's evenness), with more species evenness found in the arable soils than soils under native prairie (Figure 4c). In the B horizon, land use had a similar effect on the bacteria Faith's phylogenetic diversity compared to the A horizon but enhanced species evenness in the native prairie soils compared to soils under arable land use. In the C horizon, the bacteria Faith's phylogenetic diversity was significantly higher in the native prairie soils than in the arable soils. However, species distribution was similar in both land use systems. In contrast, fungi Faith's phylogenetic diversity and species distribution for the individual horizons were not significantly affected by land use (Figure 4d and e).

Correlations between soil organic carbon characteristics and soil chemical, physical, and biological characteristics

To identify potential factors significantly affecting SOC retention and persistence, Pearson correlation matrices were generated for the A, B, and C horizons under arable and native prairie land use (Figure S2a-f). Only significant correlations ($p < 0.05$) are considered below. Except for pH, $\delta^{13}C$ (‰), and $\Delta^{14}C$ (‰), the parameters used within the correlation analyses were bulk soil contents in mg kg^{-1} or g kg^{-1}.

Generally, a significant correlation between SOC and N_t was observed across the individual horizons regardless of land use type. For the A horizon, the SOC of arable soils was positively correlated with Al_{AO} ($r = 0.35$, $n = 33$), $\delta^{13}C$ ($r = 0.43$, $n = 33$), phosphate-P ($r = 0.53$, $n = 33$), sulfate-S ($r = 0.47$, $n = 33$), and microbial DNA ($r = 0.43$, $n = 20$) (Figure S2a). A negative correlation in arable topsoil was also detected between $\Delta^{14}C$ and Fe_{DCB} ($r = -0.89$, $n = 9$). For the native prairie soils, SOC was positively correlated with silt ($r = 0.66$, $n = 33$), exchangeable Ca ($r = 0.41$, $n = 33$), Fe_{AO} ($r = 0.56$, $n = 33$), Al_{AO} ($r = 0.53$, $n = 33$), Fe_{DCB} ($r = 0.52$, $n = 33$), and Al_{DCB}

(r = 0.61, n = 33) (Figure S2b). Furthermore, SOC was positively correlated with microbial DNA (r = 0.48, n = 19) and sulfate-S (r = 0.44, n = 33), and $\Delta^{14}C$ was negatively correlated with Fe_{AO} (r = -0.78, n = 10).

For the B horizon under arable land use, SOC showed positive correlations with silt (r = 0.35, n = 40), Al_{AO} (r = 0.33, n = 40), and microbial DNA (r = 0.54, n = 22) (Figure S2c). Under native prairie land use, similar parameters as observed for the arable soils, such as Al_{AO} (r = 0.35, n = 41) and microbial DNA (r = 0.42, n = 22), were positively correlated with SOC (Figure S2d).

For the C horizon, significant relationships between SOC or $\Delta^{14}C$ and soil mineral characteristics were not observed for the arable soils (Figure S2e). However, SOC was positively correlated with microbial DNA (r = 0.36, n = 48). For the native prairie soils, SOC was positively correlated with silt (r = 0.37, n = 80), exchangeable Ca (r = 0.32, n = 80), and Mg (r = 0.28, n = 80), Al_{AO} (r = 0.26, n = 80), and microbial DNA (r = 0.34, n = 52) (Figure S2f).

Independent of land use type and horizons-specific correlation analysis, results from the SEM indicated that management intensity negatively affected SOC through microbial DNA (Figure S3). For instance, if management intensity increases by 1.00 unit, it will cause a 0.17 unit decrease in microbial DNA, and a 1.00 unit decrease in microbial DNA will lead to a 0.51 unit decrease in SOC ($p < 0.05$). Increasing soil pH decreased Al_{AO}, Fe_{AO}, Al_{DCB}, and Fe_{DCB} ($p < 0.05$). The Al_{AO} and Fe_{AO} increased SOC ($p < 0.05$), but Al_{DCB} or Fe_{DCB} had no significant effect on SOC ($p > 0.05$).

Discussion

Land use affected soil organic carbon storage only in the A horizon or uppermost 50 cm

In the A horizon, significant differences in SOC and N_t stocks between arable and native prairie soils suggest an average loss of about 2.7 kg m^{-2} SOC (~ 34%) and 0.2 kg m^{-2} N (~ 29%) due to the intensification of land use. In most cultivated soils, topsoil SOC and N_t stocks are lower relative to undisturbed native grassland soils. This disparity can be attributed to reduced carbon inputs from annual crops, characterized by short-growing cycles and shallow root architecture, in contrast to perennial grasses with extensive root systems that contribute continuously to soil carbon (Chen et al., 2022). Additionally, the lower SOC stocks may result from increased microbial decomposition of SOC due to disruption of aggregates or topsoil SOC losses due to erosion (for example, Wiesmeier et al., 2019; Borrelli et al., 2017; Berhe et al., 2018). Previous studies conducted across the U.S. Midwest and the Great Plains have reported similar SOC losses from topsoils under cultivation, as found in our study. In a study analyzing one site in Wisconsin, Jelinski and Kucharik (2009) reported an average loss of 2.4 kg m^{-2} SOC (~35%) and 0.17 kg m^{-2} N_t from the A horizon (0-10 cm depth) of soil under long-term arable land use (~ 60 years) by comparison to an adjacent soil under native prairie land use. Liebig et al. (2009) analyzed soils from 42 sites across the U.S. Great Plains (North Dakota, Montana, Wyoming, Colorado, Kansas, Nebraska, Texas) and found an average loss of about 42% in SOC from near-surface soil (average depth of 30.5 cm) in long-term arable sites (30-120 years) relative to sites under native prairie. In the B and C horizons (i.e., subsoil horizons), our study showed no significant effect of land use on SOC and N_t stocks, suggesting that losses due to cultivation mainly impacted the surface horizon but did not extend into the subsoil horizons. Similarly, Wiesmeier et al. (2013a) did not detect land use effects on SOC storage in B and C horizons by comparing clay-rich agricultural soils in

478 Bavaria, Germany, to native grassland soils. However, A horizon depths can vary largely between
479 land use types (as shown in Table 1), soil types, and study sites, which makes it difficult to identify
480 specific soil depths that might need to be sampled and analyzed preferentially to account for the
481 majority of SOC losses due to disturbances or SOC gains due to improved management. To
482 address this, we also analyzed differences in SOC and N_t stocks for fixed depth increments.

483 The fixed depth increments analyzed here integrate information from the relative contributions
484 of different pedogenetic horizons specifically quantified for each arable and native prairie soil
485 profile. Significant differences in SOC and N_t stocks between land use types were observed in 0-
486 50 cm depth, with lower SOC and N_t stocks found in the arable soils. Our data suggest here an
487 average loss of about 2.9 kg m^{-2} SOC and 0.3 kg m^{-2} N_t due to land use change. In Northwestern
488 Illinois, Olson and Gennadiev (2020) found slightly lower SOC differences (~ 2.41 kg m^{-2}) at 0-
489 50 cm depth by comparing arable soil more than 150 years after conversion to a soil under native
490 vegetation. In a study conducted in Switzerland by Guillaume et al. (2022), on average, found 3.0
491 ± 0.8 kg m^{-2} less SOC down to 50 cm depth of arable soils compared to soils under permanent
492 grassland.

493 In contrast to other studies, we were also able to analyze differences in depth increments across
494 50 to 300 cm depth. No significant differences in SOC and Nt stocks between the two land use
495 types were detected for 50-100 cm, 100-200 cm, and 200-300 cm increments. This suggests that
496 losses due to cultivation were limited to the uppermost 50 cm soil depth, which consists of the A
497 horizon but can also include proportions of B and C horizons depending on their site-specific
498 thickness. This also highlights the need to sample soils at least 50 cm deep to capture the soil
499 volume reflecting most of the changes in SOC storage derived from changes in management or
500 land use. In line with our observations, results from ten long-term experiments in Germany

published by Skadell et al. (2023) showed significant impacts of agricultural management on SOC stocks down to 50 cm depth. In their study, the topsoil (0-30 cm) accounted for 79% of the total management effects, the upper subsoil (30-50 cm) for 19%, and the lower subsoil (50-100 cm) for 3%. Our study, which analyzed the uppermost 3 m of soil, revealed that the main impact of land use change on SOC storage was restricted to the top 50 cm. Storage-wise, our data also showed substantial amounts of SOC stored below 50 cm (57-67%), 1 m (37-45%), and even 2 m (16-19%) depth (Figure 3a, Figure S5). This highlights the significance of SOC stored at greater depths, which should be taken into consideration when budgeting for terrestrial carbon storage.

Bulk soil organic carbon is correlated to soil nutrients and microbial DNA depending on the horizon and land use

Soils under arable and native prairie showed distinct ranges in mineral characteristics (e.g., Fe_{AO}, $Al_{AO,}$ Fe_{DCB}, Al_{DCB}, exchangeable Ca, and clay content: Tables 1 to 3) known to be relevant for SOC retention (e.g., Rasmussen et al., 2018; Heckman et al., 2021; Hall and Thompson, 2021). For the A horizon of arable soils (11 sites), the amount of poorly crystalline Al-oxides (Al_{AO}) was the only mineral characteristic significantly related to SOC. In contrast, in the A horizon of native prairie soils (11 sites), contents of silt, exchangeable Ca ions, and Fe and Al oxides/hydroxides (Fe_{AO}, $Al_{AO,}$ Fe_{DCB}, and Al_{DCB}) were positively correlated with SOC. These results suggest a stronger influence of soil mineral characteristics on soil carbon retention in topsoils under native prairie compared to soils under arable land use.

For arable soils, the effects of management practices seem to mask the impact of soil minerals or are more relevant for the topsoil SOC storage than soil mineral characteristics (An et al., 2023; Xiao et al., 2023). Differences in tillage intensity, for example, are known to affect SOC levels,

especially in the topsoil (Cui et al., 2024). The SOC content of the arable soils is, for example, positively correlated with phosphate-P, suggesting an indirect effect of fertilization via enhanced crop productivity and higher soil carbon inputs from crop residues (Hijbeek et al., 2019). Crop productivity and resulting soil carbon inputs in drought-affected agro-ecoregions, as given for our study sites, are also affected by irrigation, which was used for six of our study sites (Dai, 2011; Reichstein et al., 2013). Regular high moisture events caused by irrigation can increase the occurrence of anoxic microsites in soils (Malakar et al., 2022), which can enhance the reductive dissolution of Fe-oxides relative to Al-oxides due to the biogeochemical transformation of Fe^{3+} to Fe^{2+} (e.g., Barcellos et al., 2018; Malakar et al., 2022; Li et al., 2023). In this scenario, the reductive dissolution of Fe might weaken organo-Fe complexes, thereby reducing SOC protection against microbial decomposition (Hall et al., 2018; Hall and Thompson, 2020) relative to the Al species, which is not redox-sensitive. This might explain the effect of Al_{AO} on SOC detected in the arable soils (Figure S2a), which is consistent with other studies (Rasmussen et al., 2018; Yu et al., 2021).

For the B and C horizons (11 sites for each land use type), correlations between SOC and soil characteristics were highly variable without consistent patterns. In the B horizon, Al_{AO} was the primary mineral characteristic correlated with SOC content in arable and native prairie soils, highlighting the importance of poorly crystalline Al-oxides/hydroxides for subsoil SOC retention across land use types (Hall and Thompson, 2021). In the C horizon, SOC retention was not directly linked to soil mineral characteristics in the arable soils but was positively correlated with silt, exchangeable Ca and Mg, and Al_{AO} in the native prairie soils. Overall, as assessed by correlation analyses, the controlling effect of soil mineral characteristics on subsoil SOC (i.e., B and C horizons) was lower than expected (i.e., less relationship). It is assumed that with increasing soil depth, organic compounds become smaller and more reactive towards charged mineral surface

547 sites because of the ongoing oxidative breakdown (microbial processing) (Kleber et al. 2015).
548 Consequently, with increasing soil depth, organo-mineral associations should become increasingly
549 important for SOC retention (Rasse et al. 2006). Preferential flow paths of dissolved OC and the
550 spatial discontinuity, variability, and heterogeneity of "OM-mineral interaction events" likely
551 make it difficult to detect linear relationships with individual mineral parameters in the subsoil.
552 The bulk SOC, as analyzed here, however, consists of different sub-compartments with distinct
553 soil ecological functions, such as dissolved, particulate, and mineral-associated organic
554 compounds (Anuo et al., 2023). To better understand the relevance of individual soil mineral
555 characteristics on subsoil SOC retention, the separation and quantification of mineral-associated
556 SOC seem to be necessary (Vormstein et al., 2020).

557 Independent of soil depth/horizon and land use type, SOC was positively correlated with the
558 microbial DNA content (data from 10 sites for each land use type), which serves as a proxy for
559 microbial biomass (Gong et al., 2021). The correlation can be interpreted in both directions with
560 higher substrate (i.e., SOC), resulting in higher microbial biomass. On the other hand, microbial
561 necromass and microbial decomposition products retained in soil due to associations with soil
562 minerals, for example, have been identified as major contributors to SOC formation and storage
563 (Liang et al., 2019). The impact of microbial-derived SOC on the bulk SOC should thereby
564 increase with more favorable environmental conditions for microbial communities across the soil
565 profiles in terms of habitat (i.e., pores) and resources (i.e., water, redox partners, nutrients) besides
566 organic substrate (Kästner & Miltner, 2018; Wang et al., 2021; Sokol et al., 2022). Accordingly,
567 we found higher SOC stocks and higher microbial DNA contents for the A horizon of native prairie
568 soils than for the A horizon of arable soils. This is further elucidated by our SEM results, which
569 indicate that increased management intensity exerts a deleterious effect on SOC storage overall

570 (Figure S3). This negative impact likely results in diminished SOC stocks and reduced microbial
571 biomass in the more intensively managed arable soils relative to the undisturbed native soils.
572
573
574 *Persistence of soil organic carbon increased with soil depth but was affected by land use only in*
575 *the A horizon*
576 Bulk soil $\delta^{13}C$ and $\Delta^{14}C$, which provided more information on SOC turnover and persistence
577 within the analyzed land use systems, decreased with soil depth (Figure 2 c and d; Table 4). The
578 $\delta^{13}C$ values were not affected by the type of land use, although our study sites have experienced a
579 complex vegetation history, including the presence of C_3 and C_4 plants. The decrease in $\delta^{13}C$ with
580 depth might be explained by differences across horizons in C_4 derived carbon inputs (here: Process
581 1) and with differences in the amount of organic matter highly microbially processed (here:
582 Process 2).
583 For Process 1, soil $\delta^{13}C$ values of -22 to -32 ‰ generally indicate carbon input from C_3 plants,
584 whereas values of -12 to -17 ‰ suggest carbon input from C_4 plants whose biomass is ^{13}C enriched,
585 leading to less negative $\delta^{13}C$ values as compared with C_3 plants (Malo et al., 2005; Slessarev et
586 al., 2020). In the A horizon, average bulk soil $\delta^{13}C$ values of -15.8 ‰ (arable soils) and -16.2 ‰
587 (prairie soils) were found, suggesting C_4-derived carbon inputs for both land use systems. For the
588 arable soils, the C_4-carbon originates from corn (Malo et al., 2005), and for the native prairie soils
589 from C_4-grasses (Havrilla et al., 2022). In the B horizon, a slight decline in the average $\delta^{13}C$ values
590 (-17.9 and 17.2 ‰) compared to the A horizon indicates material with a lower ^{13}C abundance and
591 less C_4 plant derived carbon input. This trend is even stronger in the C horizon, where average

592 $\delta^{13}C$ values of -21.4 and -22.3 ‰ were observed. This suggests that the SOC in the C horizon is
593 dominated by C_3 derived carbon.

594 For Process 2, it is known that microorganisms preferentially metabolize the lighter ^{12}C, thus
595 enriching the heavier ^{13}C isotope and leading to less negative $\delta^{13}C$ values in organic matter not
596 fully processed/respired and retained in the soil (Balesdent et al., 2018). The decreasing microbial
597 DNA content with depth (Figure 4a) points towards an accompanied decrease in microbial
598 abundance and decomposition activity. This, in turn, seems to contribute to the decrease in $\delta^{13}C$
599 found for the A, B, and C horizons due to decreasing amounts of highly microbially processed
600 organic matter and ^{13}C enriched with depth (Scheibe et al., 2023). Specifically for the C horizons,
601 the most negative $\delta^{13}C$ values suggest low input of C_4 derived carbon, low microbial processing
602 of organic matter, and low input of microbially processed organic matter mobilized in the A and
603 B horizons and translocated into the C horizon (Sanderman et al., 2008; Kaiser and Kalbitz, 2012).

604 The information obtained from $\Delta^{14}C$ can offer a better understanding in order to untangle the
605 patterns observed above. The ^{14}C analyses showed that land use affected the $\Delta^{14}C$ value in the A
606 horizon, with less depleted (younger) $\Delta^{14}C$ observed in the native prairie soils compared to the
607 arable soils (Figure 2d and Table 4). It appears that the A horizon has experienced a preferential
608 loss of more recently incorporated and potentially less protected organic material due to the
609 conversion of native prairie vegetation into arable land (Finstad et al., 2019). This loss appears to
610 have resulted in the preservation of older and more stabilized organic materials leading to a higher
611 mean residence time as inferred from the $\Delta^{14}C$ values (Table 4). A similar observation was
612 reported by Mikhailova et al. (2018) in the Russian Chernozem with more depleted (older) $\Delta^{14}C$
613 in arable soil relative to soil under native grassland. Our finding that the $\Delta^{14}C$ values were
614 negatively correlated with Fe_{DCB} for the arable soils (9 sites) and with Fe_{AO} for the native prairie

soils (10 sites) (Figure S2a and b) indicates stronger stabilization of organic matter against microbial decomposition in the topsoil with increasing content of Fe-oxides/hydroxides. Here, more crystalline, and less redox-sensitive Fe-species (i.e., Fe_{DCB}) seem more relevant in the arable soils than the native prairie soils. Direct evidence beyond the performed correlation analyses to prove the assumption that older OC is more stabilized against microbial decay would require extended decomposition experiments coupled with $^{14}CO_2$ measurements to track the origin of respired carbon, which is not within the scope of this study.

In the B horizon, no significant differences in the $\Delta^{14}C$ values were observed between the land use systems. However, the $\Delta^{14}C$ of SOC in the B horizon of native prairie soils (-380 ± 83‰) was substantially less negative than in arable soils (-518 ± 75‰), showing a similar pattern as the A horizon. Typically, native prairie soil receives a higher continuous input of recently assimilated OC via plant roots and root exudates as opposed to arable soils, which are often more disturbed with higher microbial decomposition rates leading to less recent or fresh carbon (Hauser et al., 2022) (i.e., more depleted or negative $\Delta^{14}C$ values). The absence of a significant difference in $\Delta^{14}C$ between arable and native grassland soil in the B horizon can result from a generally lower disturbance sensitivity of the subsoil compared to the topsoil. Another factor can be the higher depth span for the B horizon compared to the A horizon, which would increase the variability for the B horizon data, making more data (study sites) necessary to detect significant differences.

Independent of land use effect, the $\Delta^{14}C$ values were more negative in the B horizon than the values detected in the A horizon. This suggests an accumulation of more persistent SOC with depth, which is not affected by land use. Paul et al. (2001) found similar trends with depth for SOC-$\Delta^{14}C$ analyses with ^{14}C age in the range of 485 - 1100 years BP in the surface horizon (0-20 cm) of two arable soils derived from grassland soils in the U.S. Midwest compared to 2620 - 3100

638 years BP in 25-50 cm depth, and 4412 -6107 years BP in 50-100 cm depth. Overall, the strong
639 negative $\Delta^{14}C$ values point towards soil environmental conditions in the B horizons, promoting the
640 long-term persistence of carbon in this subsoil compartment. Based on the soil $\delta^{13}C$ values (-17.9
641 and -17.2‰), this carbon might be derived from less microbially processed and stabilized C_4-plant
642 compounds (^{13}C enriched), highly microbially processed C_3-plant compounds (^{13}C enriched),
643 and/or from stabilized microbial biomass (^{13}C enriched, Coyle et al., 2009).

644 In the C horizon, an average $\Delta^{14}C$ of -746 ± 33‰ was detected for the arable soils, which was
645 very similar to the $\Delta^{14}C$ of -730 ± 38‰ observed for the native prairie soils. Strong depletion in
646 $\Delta^{14}C$ at 3 m and deeper was previously reported by Moreland et al. (2021). Our findings indicate
647 that the SOC persistence continued to drastically increase with depth along pedogenetic boundary
648 conditions that resulted in the formation of A, B, and C horizons independent of the land use
649 system. The $\delta^{13}C$ values (-21.4, -22.3 ‰) indicate that the organic material in the C horizon was
650 mainly derived from highly stabilized C_3-plant compounds. An explanation could be that this
651 material was derived and preserved from the early stages of soil development and revegetation
652 preceding the last ice age (glacial retreat) (Van Der Voort et al., 2019). Based on historical records,
653 it is widely recognized that C_3 grasses were the dominant vegetation in grassland eco-regions
654 characterized by lower temperatures and varying precipitation levels (Havrilla et al., 2022). It is
655 probable that during early soil development stages approximately 12,000 years ago (based on
656 average conventional ^{14}C radiocarbon age) (Figure S6), the predominant vegetation consisted of
657 C_3 species (Edwards et al., 2017).

658 The similar and strong negative $\Delta^{14}C$ and $\delta^{13}C$ values found in this study for the C horizons of
659 soils under arable and native prairie land use suggest this pedogenetically defined soil environment
660 to be less affected by inputs of recently assimilated carbon and OC translocation and

transformation processes that seem to be more important for SOC storage and turnover in A and B horizons. However, the intensity of subsoil OC responses to changes in management seem to be affected by site-specific characteristics such as texture (Slessarev et al., 2020) or management strategy (Tautges et al., 2019), which might not be reflected in the average values across sites as presented here. Inputs from recently assimilated carbon into the deeper subsoil (i.e., below B horizon) via roots or dissolved OC might serve immediately as substrate for the subsoil microorganisms, thereby reducing the imprint of these inputs on bulk soil $\Delta^{14}C$ and $\delta^{13}C$ values (Scheibe et al., 2023). This also implies that, especially for the C horizon, more research is needed to clarify if and how this soil compartment can play a significant role in increasing long-term carbon storage across the soil profile.

Soil microbial abundance decreased with depth, but community structure was differentially affected by land use within individual horizons

At the community level, the diversity of bacteria and fungi (Faith's phylogenetic diversity) decreased with depth (Figure 4b and d). The highest diversity was observed in the topsoil horizon (A horizon), while the subsoil horizons (B and C horizons) had lower diversity independent of land use type. Polain et al. (2020) and Upton et al. (2020) found a similar trend in a 1 m deep soil profile under arable land use and native grassland, respectively. In their study, the authors found that both bacteria and fungi diversity decreased with increasing soil depth. The microbial diversity (bacteria and fungi) observed in our study followed a similar trend as the microbial DNA concentration (an indicator of microbial biomass) (Figure 4a; Gong et al., 2021), which positively correlated with SOC content across the individual horizons (Figure S2a-f). In line with this observation, Bastida et al. (2021) found that increased SOC content significantly enhanced soil

684 microbial biomass, influencing the diversity of bacteria and fungi communities. Moreover, studies
685 have shown that substrate availability plays a crucial role in regulating the diversity of soil
686 microorganisms under different land use systems (Chen et al., 2022; Han et al., 2023). Thus,
687 variation in substrate accessibility due to differences in land use types and across depth or horizon
688 can affect microbial resources (e.g., carbon, nitrogen, phosphorus, sulfur) (Han et al., 2023),
689 consequently driving changes in community patterns (i.e., distribution) and composition
690 (Labouyrie et al., 2023).

691 Although there were no significant changes in the diversity of bacteria and fungi communities
692 between arable and native prairie soils in the A horizon, the arable soils had a higher degree of
693 species evenness (Pielou evenness) within the bacteria community compared to soils under native
694 prairie (Figure 4c). This observation indicates a relatively balanced distribution among species in
695 the arable soils, most likely due to a broader array of resources (Romdhane et al., 2022). For
696 example, studies have shown that agricultural intensification enhanced bacterial diversity in the
697 topsoil, due to rotations of different crop types and changes in management practices (e.g.,
698 fertilization) that may result in higher substrate diversity via root, crop residues, and legacy effect
699 of nutrients (Delgado-Baquerizo et al., 2016; Romdhane et al., 2022). Furthermore, increased
700 niche availability in arable soils due to soil disturbance or the existence of a heterogeneous
701 environment with different crop species may result in higher microbial diversity (Labouyrie et al
702 2023).

703 Similar to the A horizon, the diversity of bacteria and fungi communities in the B horizon was
704 not affected by land use. However, within the bacteria community, greater species distribution was
705 observed in soils under native prairie compared to soils under arable land use (Figure 4c). Since
706 grassland vegetation consists of perennial plants that continuously contribute to subsoil SOC via

roots and root exudates (Bai & Cotrufo, 2022), substrate derived from perennial roots, which extend even up to 2 meters in the native prairie soils studied here, may play a significant role. In contrast, arable soils are typically cultivated with annual crops with short growing cycles that can limit the amount of OC inputs into the subsoil (Salonen et al., 2023).

In the C horizon, land use only affected the diversity of the bacteria community, with higher diversity observed in the native prairie soils compared to arable soils. This observation further strengthens the hypothesis that alterations in microbial communities in the subsoil could be impacted by inputs originating from perennial roots (Upton et al., 2020).

Conclusions

Most of the SOC losses due to increased agricultural intensification of native prairie ecosystems seem to be restricted to the uppermost 50 cm, which might be targeted in future studies as the minimum sampling depth needed to account for changes in SOC due to changed management or land use. Relationships between SOC and soil mineral characteristics varied depending on soil horizon and land use type. Oxalate soluble Al was positively correlated to SOC in almost all combinations of soil horizon and land use type, while clay content was not correlated with SOC for any of the analyzed soil environments. This suggests soil mineral characteristics other than clay content might be more important for predicting soil carbon storage under changing soil environmental conditions.

For both land use systems, $\delta^{13}C$ and $\Delta^{14}C$ decreased with soil depth along pedogenetic boundary conditions that resulted in the formation of A, B, and C horizons. The strong negative and very similar $\delta^{13}C$ and $\Delta^{14}C$ values found for the SOC of the C horizons for both land use types suggest these carbon pools to be less affected by inputs from recently assimilated carbon.

However, the increase in bacteria diversity found in the C horizon of native prairie soils as compared to arable soils suggests that changes in microbial diversity may have been influenced by inputs from perennial roots. These findings support previously postulated subsoil carbon pathways (Scheibe et al., 2023), where subsoil inputs of recently assimilated carbon are preferentially used as substrate by microorganisms populating the deeper subsoil (i.e., below B horizon). Overall, our study suggests that the impact of land use change on SOC storage is not solely horizon-dependent but also depth-dependent since the uppermost 50 cm may include A, B, and C horizons based on their thickness.

Acknowledgments

Our thanks go out to Dr. Rebecca Young for providing soil pedology expertise during soil sample diagnostic characterization and horizon designation. We thank Aaron Hird at Natural Resources Conservation Service for helping with information on sites in different Major Land Resource Areas (MLRAs) in Nebraska.

This work was supported in part by the U.S. Department of Agriculture Natural Resources Conservation Service (USDA-NRCS) with grant number (NR206526XXXXC037). A portion of this work was performed under the auspices of the U.S. Department of Energy by Lawrence Livermore National Laboratory under Contract DE-AC52-07NA27344.

Data Availability

The datasets generated during and/or analyzed during the current study are archived on GitHub (https://github.com/chrisanuo/Raw-data).

Declarations

The authors declare that they have no known competing financial interests or personal relationships that could have appeared to influence the work reported in this paper.

References

Amelung, W., Bossio, D., de Vries, W., Kögel-Knabner, I., Lehmann, J., Amundson, R., Bol, R., Collins, C., Lal, R., Leifeld, J., Minasny, B., Pan, G., Paustian, K., Rumpel, C., Sanderman, J., van Groenigen, J. W., Mooney, S., van Wesemael, B., Wander, M., & Chabbi, A (2020) Towards a global-scale soil climate mitigation strategy. Nature Communications, 11(1), 1–10. https://doi.org/10.1038/s41467-020-18887-7

An, Z., Pokharel, P., Plante, A. F., Bork, E. W., Carlyle, C. N., Williams, E. K., & Chang, S. X (2023) Soil organic matter stability in forest and cropland components of two agroforestry systems in western Canada. Geoderma, 433(March), 116463. https://doi.org/10.1016/j.geoderma.2023.116463

Angst, G., Messinger, J., Greiner, M., Häusler, W., Hertel, D., Kirfel, K., Kögel-Knabner, I., Leuschner, C., Rethemeyer, J., & Mueller, C. W (2018) Soil organic carbon stocks in topsoil and subsoil controlled by parent material, carbon input in the rhizosphere, and microbial-derived compounds. Soil Biology and Biochemistry, 122, 19–30. https://doi.org/10.1016/j.soilbio.2018.03.026

Anuo, C. O., Cooper, J. A., Koehler-Cole, K., Ramirez, S., & Kaiser, M (2023) Effect of cover cropping on soil organic matter characteristics: Insights from a five-year field experiment in Nebraska. Agriculture, Ecosystems and Environment, 347. https://doi.org/10.1016/j.agee.2023.108393

Bai, Y., & Cotrufo, M. F (2022) Grassland soil carbon sequestration: Current understanding, challenges, and solutions. Science, 377(6606), 603–608. https://doi.org/10.1126/science.abo2380

798 Balesdent, J., Basile-Doelsch, I., Chadoeuf, J., Cornu, S., Derrien, D., Fekiacova, Z., & Hatté, C
799 (2018) Atmosphere–soil carbon transfer as a function of soil depth. Nature, 559(7715),
800 599–602. https://doi. org/10.1038/s41586-018-0328-3
801 Barcellos, D., O'Connell, C. S., Silver, W., Meile, C., & Thompson, A (2018) Hot spots and hot
802 moments of soil moisture explain fluctuations in iron and carbon cycling in a humid tropical
803 forest soil. Soil Systems, 2(4), 59. https://doi.org/10.3390/soilsystems2040059
804 Bastida, F., Eldridge, D. J., García, C., Kenny Png, G., Bardgett, R. D., & Delgado-Baquerizo,
805 M., 2021. Soil microbial diversity–biomass relationships are driven by soil carbon content
806 across global biomes. ISME Journal, 15(7), 2081–2091. https://doi.org/10.1038/s41396-
807 021-00906-0
808 Beniston, J. W., DuPont, S. T., Glover, J. D., Lal, R., & Dungait, J. A. J (2014) Soil organic
809 carbon dynamics 75 years after land-use change in perennial grassland and annual wheat
810 agricultural systems. Biogeochemistry, 120(1–3), 37–49. https://doi.org/10.1007/s10533-
811 014-9980-3

812 Berhe, A. A., Barnes, R. T., Six, J., & Marín-Spiotta, E (2018) Role of Soil Erosion in
813 Biogeochemical Cycling of Essential Elements: Carbon, Nitrogen, and Phosphorus. Annual
814 Review of Earth and Planetary Sciences, 46, 521–548. https://doi.org/10.1146/annurev-
815 earth-082517-010018

816 Bolyen, E., Rideout, J. R., Dillon, M. R., Bokulich, N. A., Abnet, C. C., Al-Ghalith, G. A.,
817 Alexander, H., Alm, E. J., Arumugam, M., Asnicar, F., Bai, Y., Bisanz, J. E., Bittinger, K.,
818 Brejnrod, A., Brislawn, C. J., Brown, C. T., Callahan, B. J., Caraballo-Rodríguez, A. M.,
819 Chase, J., … Caporaso, J. G (2019) Reproducible, interactive, scalable and extensible

820 microbiome data science using QIIME 2. Nature Biotechnology, 37(8), 852–857.
821 https://doi.org/10.1038/s41587-019-0209-9.

822 Borrelli, P., Robinson, D. A., Fleischer, L. R., Lugato, E., Ballabio, C., Alewell, C., Meusburger,
823 K., Modugno, S., Schütt, B., Ferro, V., Bagarello, V., Oost, K. Van, Montanarella, L., &
824 Panagos, P. (2017) An assessment of the global impact of 21st century land use change on
825 soil erosion. Nature Communications, 8(1). https://doi.org/10.1038/s41467-017-02142-7

826 Broek, T. A. B., Ognibene, T. J., McFarlane, K. J., Moreland, K. C., Brown, T. A., and Bench, G
827 (2021) Conversion of the LLNL/CAMS 1 MV biomedical AMS system to a semi-
828 automated natural abundance ^{14}C spectrometer: system optimization and performance
829 evaluation, Nuclear Instruments and Methods in Physics Research Section B: Beam
830 Interactions with Materials and Atoms, 499, 124-132, 10.1016/j.nimb.2021.01.022, 2021.
831 Buée, M., Reich, M., Murat, C., Morin, E., Nilsson, R. H., Uroz, S., & Martin, F (2009) 454
832 Pyrosequencing analyses of forest soils reveal an unexpectedly high fungal diversity. New
833 Phytologist, 184(2), 449–456. https://doi.org/10.1111/j.1469-8137.2009.03003.x
834 Cagnarini, C., Blyth, E., Emmett, B. A., Evans, C. D., Griffiths, R. I., Keith, A., Jones, L.,
835 Lebron, I., McNamara, N. P., Puissant, J., Reinsch, S., Robinson, D. A., Rowe, E. C.,
836 Thomas, A. R. C., Smart, S. M., Whitaker, J., & Cosby, B. J (2019) Zones of influence for
837 soil organic matter dynamics: A conceptual framework for data and models. Global Change
838 Biology, 25(12), 3996–4007. https://doi.org/10.1111/gcb.14787
839 Callahan, B. J., McMurdie, P. J., Rosen, M. J., Han, A. W., Johnson, A. J. A., & Holmes, S. P
840 (2016) DADA2: High-resolution sample inference from Illumina amplicon data. Nature
841 Methods, 13(7), 581–583. https://doi.org/10.1038/nmeth.3869

842 Caporaso, J. G., Lauber, C. L., Walters, W. A., Berg-Lyons, D., Huntley, J., Fierer, N., Owens,
843 S. M., Betley, J., Fraser, L., Bauer, M., Gormley, N., Gilbert, J. A., Smith, G., & Knight, R
844 (2012) Ultra-high-throughput microbial community analysis on the Illumina HiSeq and
845 MiSeq platforms. ISME Journal, 6(8), 1621–1624. https://doi.org/10.1038/ismej.2012.8
846 Caporaso, J. G., Lauber, C. L., Walters, W. A., Berg-Lyons, D., Lozupone, C. A., Turnbaugh, P.
847 J., Fierer, N., & Knight, R (2011) Global patterns of 16S rRNA diversity at a depth of
848 millions of sequences per sample. Proceedings of the National Academy of Sciences of the
849 United States of America, 108(SUPPL. 1), 4516–4522.
850 https://doi.org/10.1073/pnas.1000080107
851 Chabbi, A., Kögel-Knabner, I., & Rumpel, C (2009) Stabilised carbon in subsoil horizons is
852 located in spatially distinct parts of the soil profile. Soil Biology and Biochemistry, 41(2),
853 256–261. https://doi.org/10.1016/j.soilbio.2008.10.033

854 Chen, J., Lærke, P. E., & Jørgensen, U (2022) Land conversion from annual to perennial crops:
855 A win-win strategy for biomass yield and soil organic carbon and total nitrogen
856 sequestration. Agriculture, Ecosystems and Environment, 330(September 2021).
857 https://doi.org/10.1016/j.agee.2022.107907

858 Chen, Q., Yang, F., & Cheng, X (2022) Effects of land use change type on soil microbial
859 attributes and their controls: Data synthesis. Ecological Indicators, 138(March), 108852.
860 https://doi.org/10.1016/j.ecolind.2022.108852
861 Cotrufo, M.F., and Lavallee, J.M (2022) Soil organic matter formation, persistence, and
862 functioning: A synthesis of current understanding to inform its conservation and

regeneration. Advances in Agronomy, 172, 1-66. https://doi.org/10.1016/bs.agron.2021.11.002

Cotrufo, M.F., Wallenstein, M.D., Boot, C.M., Denef, K., Paul, E (2013) The Microbial Efficiency-Matrix Stabilization (MEMS) framework integrates plant litter decomposition with soil organic matter stabilization: do labile plant inputs form stable soil organic matter? Global Change Biology 19, 988–995. https://doi.org/ 10.1111/gcb.12113.

Coyle, J. S., Dijkstra, P., Doucett, R. R., Schwartz, E., Hart, S. C., & Hungate, B. A (2009) Relationships between C and N availability, substrate age, and natural abundance 13C and 15N signatures of soil microbial biomass in a semiarid climate. Soil Biology and Biochemistry, 41(8), 1605–1611. https://doi.org/10.1016/j.soilbio.2009.04.022

Cui, Y., Zhang, W., Zhang, Y., Liu, X., Zhang, Y., Zheng, X., Luo, J., & Zou, J. (2022). Effects of no-till on upland crop yield and soil organic carbon: a global meta-analysis. Plant and Soil, 499(1), 363–377. https://doi.org/10.1007/s11104-022-05854-y

Dai, A (2011) Drought under global warming: A review. Wiley Interdisciplinary Reviews: Climate Change, 2(1), 45–65. https://doi.org/10.1002/wcc.81

Delgado-Baquerizo, M., Maestre, F. T., Reich, P. B., Jeffries, T. C., Gaitan, J. J., Encinar, D., Berdugo, M., Campbell, C. D., & Singh, B. K., 2016. Microbial diversity drives multifunctionality in terrestrial ecosystems. Nature Communications, 7, 1–8. https://doi.org/10.1038/ncomms10541

Dijkstra, F. A., Zhu, B., & Cheng, W (2021) Root effects on soil organic carbon: a double-edged sword. New Phytologist, 230(1), 60–65. https://doi.org/10.1111/nph.17082

884 Doane, T. A., & Horwáth, W. R (2003) Spectrophotometric determination of nitrate with a single
885 reagent. Analytical Letters, 36(12), 2713–2722. https://doi.org/10.1081/AL-120024647
886 Edwards, K. J., Fyfe, R. M., & Jackson, S. T (2017) The first 100 years of pollen analysis.
887 Nature Plants, 3(2). https://doi.org/10.1038/nplants.
888 Ellert, B. H., Janzen, H. H., & Entz, T (2002) Assessment of a Method to Measure Temporal
889 Change in Soil Carbon Storage. Soil Science Society of America Journal, 66(5), 1687–
890 1695. https://doi.org/10.2136/sssaj2002.1687
891 Finstad, K., van Straaten, O., Veldkamp, E., & McFarlane, K (2020) Soil Carbon Dynamics
892 Following Land Use Changes and Conversion to Oil Palm Plantations in Tropical Lowlands
893 Inferred from Radiocarbon. Global Biogeochemical Cycles, 34(9).
894 https://doi.org/10.1029/2019GB006461

895 Fierer, N., Ladau, J., Clemente, J. C., Leff, J. W., Owens, S. M., Pollard, K. S., Knight, R.,
896 Gilbert, J. A., & McCulley, R. L (2013). Reconstructing the microbial diversity and
897 function of pre-agricultural tallgrass prairie soils in the United States. Science, 342(6158),
898 621–624. https://doi.org/10.1126/science.1243768

899 Follett, R. F., Stewart, C. E., Pruessner, E. G., & Kimble, J. M (2012) Effects of climate change
900 on soil carbon and nitrogen storage in the US Great Plains. Journal of Soil and Water
901 Conservation, 67(5), 331–342. https://doi.org/10.2489/jswc.67.5.331
902 Franzluebbers, A. J (2021) Root-zone enrichment of carbon, nitrogen, and soil-test biological
903 activity under cotton systems in North Carolina. Soil Science Society of America Journal,
904 85(5), 1785–1798. https://doi.org/10.1002/saj2.20290

905 Gee, G.W. and D. Or (2002) Particle-size analysis: In Dane, J.H. and G.C. Topp (eds.), Methods
906 of Soil Analysis, Part 4. Physical Methods, Soil Science Society of America Book Series
907 no. 5. p. 255-293
908 Gong, H., Du, Q., Xie, S., Hu, W., Akram, M. A., Hou, Q., Dong, L., Sun, Y., Manan, A., Deng,
909 Y., Ran, J., & Deng, J (2021) Soil microbial DNA concentration is a powerful indicator for
910 estimating soil microbial biomass C and N across arid and semi-arid regions in northern
911 China. Applied Soil Ecology, 160(December 2020).
912 https://doi.org/10.1016/j.apsoil.2020.103869
913 Grossman, R.B., and T.G. Reinsch (2002) Bulk density and linear extensibility. In: Dane, J.H.,
914 Topp, G.C. (Eds.), Methods of Soil Analysis: Part 4. Physical Methods. Book Series No. 5,
915 SSSA and ASA. Madison, WI, pp. 201–225.
916 Gross, C. D., & Harrison, R. B (2019) The case for digging deeper: Soil organic carbon storage,
917 dynamics, and controls in our changing world. Soil Systems, 3(2), 1–24.
918 https://doi.org/10.3390/soilsystems3020028
919 Guillaume, T., Makowski, D., Libohova, Z., Elfouki, S., Fontana, M., Leifeld, J., Bragazza, L.,
920 & Sinaj, S (2022) Carbon storage in agricultural topsoils and subsoils is promoted by
921 including temporary grasslands into the crop rotation. Geoderma, 422(May), 115937.
922 https://doi.org/10.1016/j.geoderma.2022.115937
923 Hall, S. J., Berhe, A. A., & Thompson, A (2018) Order from disorder: Do soil organic matter
924 composition and turnover co-vary with iron phase crystallinity? Biogeochemistry, 140, 93–
925 110. https://doi.org/10.1007/s10533-018-0476-4

926 Hall, S. J., & Thompson, A (2021) What do relationships between extractable metals and soil
927 organic carbon concentrations mean? Soil Science Society of America Journal, June 2021,
928 1–14. https://doi.org/10.1002/saj2.20343
929 Hall, S. J., Ye, C., Weintraub, S. R., & Hockaday, W. C (2020) Molecular trade-offs in soil
930 organic carbon composition at continental scale. Nature Geoscience, 13(10), 687–692.
931 https://doi.org/10.1038/ s41561-020-0634-x
932 Han, W., Wang, F., Zhang, L., Zhao, H., Zheng, Y., Sun, R., & Meng, L (2023) Variations of
933 soil bacterial community and denitrifier abundance with depth under different land-use
934 types. Journal of Soils and Sediments, 23(4), 1889–1900. https://doi.org/10.1007/s11368-
935 023-03428-8
936 Harris, D., Horwáth, W. R., & van Kessel, C (2001) Acid fumigation of soils to remove
937 carbonates prior to total organic carbon or CARBON-13 isotopic analysis. Soil Science
938 Society of America Journal, 65(6), 1853–1856. https://doi.org/10.2136/sssaj2001.1853
939 Harrison, R.B., Footen, P.W., Strahm, B.D (2011) Deep soil horizons: Contribution and
940 importance to soil carbon pools and in assessing whole-ecosystem response to management
941 and global change. Forest Science 57, 67-76.
942 Havrilla, C. A., Bradford, J. B., Yackulic, C. B., & Munson, S. M (2022) Divergent climate
943 impacts on C_3 versus C_4 grasses imply widespread 21st century shifts in grassland
944 functional composition. Diversity and Distributions, 29(3), 379–394.
945 https://doi.org/10.1111/ddi.13669
946 Hauser E, Sullivan P. L, Flores A. N, Hirmas D, Billings S. A (2022). Global-scale shifts in
947 rooting depths due to Anthropocene land cover changes pose unexamined consequences for
948 critical zone functioning. Earth's Future. 10: e2022EF002897

949 Heckman, K. A., Nave, L. E., Bowman, M., Gallo, A., Hatten, J. A., Matosziuk, L. M.,
950 Possinger, A. R., SanClements, M., Strahm, B. D., Weiglein, T. L., Rasmussen, C., &
951 Swanston, C. W (2021) Divergent controls on carbon concentration and persistence
952 between forests and grasslands of the conterminous US. Biogeochemistry, 156(1), 41–56.
953 https://doi.org/10.1007/s10533-020-00725-z
954 Hicks Pries, C. E., Sulman, B. N., West, C., O'Neill, C., Poppleton, E., Porras, R. C., Castanha,
955 C., Zhu, B., Wiedemeier, D. B., & Torn, M. S (2018) Root litter decomposition slows with
956 soil depth. Soil Biology and Biochemistry, 125(March), 103–114.
957 https://doi.org/10.1016/j.soilbio.2018.07.002
958 Hijbeek, R., van Loon, M., & van Ittersum, M (2019) Fertiliser use and soil carbon sequestration:
959 trade-offs and opportunities. CGIAR Research Program on Climate Change, Agriculture
960 and Food Security (CCAFS), 264, 12. www.ccafs.cgiar.org
961 Jelinski, N. A., & Kucharik, C. J (2009) Land-use Effects on Soil Carbon and Nitrogen on a U.S.
962 Midwestern Floodplain. Soil Science Society of America Journal, 73(1), 217–225.
963 https://doi.org/10.2136/sssaj2007.0424
964 Jobbágy, E. G., & Jackson, R. B (2000) The vertical distribution of soil organic carbon and its
965 relation to climate and vegetation. Ecological Applications, 10(2), 423–436.
966 https://doi.org/10.1890/1051-0761(2000)010 [0423: TVDOSO]2.0.CO;2
967 Kästner, M., & Miltner, A (2018) SOM and microbes—What is left from microbial life. In C.
968 Garcia, P. Nannipieri & T. Hernandez (Eds.), The future of soil carbon (pp. 125–163). San
969 Diego, CA: Academic Press. https://doi.org/10.1016/B978-0-12-811687-6.00005-5
970 Kaiser, K., and Kalbitz, K (2012) Cycling downwards–dissolved organic matter in soils, Soil
971 Biology & Biochemistry., 52, 29–32, https://doi.org/10.1016/j.soilbio.2012.04.002

Kallenbach, C.M., Frey, S.D., Grandy, A.S (2016) Direct evidence for microbial-derived soil organic matter formation and its ecophysiological controls. Nat. Commun. 7 (1) https://doi.org/10.1038/ncomms13630.

Katoh, K., Misawa, K., Kuma, K. I., & Miyata, T (2002) MAFFT: A novel method for rapid multiple sequence alignment based on fast Fourier transform. Nucleic Acids Research, 30(14), 3059–3066. https://doi.org/10.1093/nar/gkf436

Keiluweit, M., Bougoure, J. J., Nico, P. S., Pett-Ridge, J., Weber, P. K., & Kleber, M (2015). Mineral protection of soil carbon counteracted by root exudates. Nature Climate Change, 5(6), 588–595. https://doi.org/10.1038/nclimate2580

Kleber, M., Eusterhues, K., Keiluweit, M., Mikutta, C., Mikutta, R., & Nico, P. S (2015) Mineral-Organic Associations: Formation, Properties, and Relevance in Soil Environments. In Advances in Agronomy (Vol. 130). Elsevier Ltd. https://doi.org/10.1016/bs.agron.2014.10.005

Labouyrie, M., Ballabio, C., Romero, F., Panagos, P., Jones, A., Schmid, M. W., Mikryukov, V., Dulya, O., Tedersoo, L., & Bahram, M (2023) Patterns in soil microbial diversity across Europe. Nature Communications 14:3311. https://doi.org/10.1038/s41467-023-37937-4

Lal, R., 2019. Eco-intensification through soil carbon sequestration: Harnessing ecosystem services and advancing sustainable development goals. Journal of Soil and Water Conservation, 74(3), 55A-61A. https://doi.org/10.2489/jswc.74.3.55A

Li, Q., Hu, W., Li, L., & Li, Y (2023) Interactions between organic matter and Fe oxides at soil micro-interfaces: Quantification, associations, and influencing factors. Science of the Total Environment, 855(July 2022). https://doi.org/10.1016/j.scitotenv.2022.158710

994 Li, L., Wilson, C. B., He, H., Zhang, X., Zhou, F., & Schaeffer, S. M (2019). Physical,
995 biochemical, and microbial controls on amino sugar accumulation in soils under long-term
996 cover cropping and no-tillage farming. Soil Biology and Biochemistry, 135, 369–378.
997 https://doi.org/10.1016/j.soilbio.2019.05.017

998 Li, N., Zhou, S., & Margenot, A. J (2023) From prairie to crop: Spatiotemporal dynamics of
999 surface soil organic carbon stocks over 167 years in Illinois, U.S.A. Science of the Total
1000 Environment, 857. https://doi.org/10.1016/j.scitotenv.2022.159038

1001 Liang, C., Amelung, W., Lehmann, J., & Kästner, M (2019) Quantitative assessment of
1002 microbial necromass contribution to soil organic matter. Global Change Biology, 25(11),
1003 3578–3590. https://doi.org/10.1111/gcb.14781
1004 Liebig, M. A., Mikha, M. M., & Potter, K. N (2009) Management of dryland cropping systems in
1005 the U.S. great plains: Effects on soil organic carbon. Soil Carbon Sequestration and the
1006 Greenhouse Effect, 97–113. https://doi.org/10.2136/sssaspecpub57.2ed.c6
1007 Maharjan, B., Das, S., & Acharya, B. S (2020) Soil Health Gap: A concept to establish a
1008 benchmark for soil health management. Global Ecology and Conservation, 23, e01116.
1009 https://doi.org/10.1016/j.gecco.2020.e01116

1010 Mackelprang, R., Grube, A. M., Lamendella, R., Jesus, E. da C., Copeland, A., Liang, C.,
1011 Jackson, R. D., Rice, C. W., Kapucija, S., Parsa, B., Tringe, S. G., Tiedje, J. M., & Jansson,
1012 J. K (2018). Microbial community structure and functional potential in cultivated and native
1013 tallgrass prairie soils of the midwestern United States. Frontiers in Microbiology, 9(AUG),
1014 1–15. https://doi.org/10.3389/fmicb.2018.01775

1015 Malakar, A., Snow, D. D., Kaiser, M., Shields, J., Maharjan, B., Walia, H., Rudnick, D., & Ray,
1016 C (2022) Ferrihydrite enrichment in the rhizosphere of unsaturated soil improves nutrient
1017 retention while limiting arsenic and uranium plant uptake. Science of the Total
1018 Environment, 806, 150967. https://doi.org/10.1016/j.scitotenv.2021.150967
1019 Mallarino, A. P (2003) Field Calibration for Corn of the Mehlich-3 Soil Phosphorus Test with
1020 Colorimetric and Inductively Coupled Plasma Emission Spectroscopy Determination
1021 Methods. Soil Science Society of America Journal, 67(6), 1928–1934.
1022 https://doi.org/10.2136/sssaj2003.1928
1023 Malo, D. D., Schumacher, T. E., & Doolittle, J. J (2005) Long-term cultivation impacts on
1024 selected soil properties in the northern Great Plains. Soil and Tillage Research, 81(2), 277–
1025 291. https://doi.org/10.1016/j.still.2004.09.015
1026 Mikhailova, E. A., Bryant, R. B., Galbraith, J. M., Wang, Y., Post, C. J., Khokhlova, O. S.,
1027 Schlautman, M. A., Cope, M. P., & Shen, Z (2018) Pedogenic carbonates and radiocarbon
1028 isotopes of organic carbon at depth in the Russian chernozem. Geosciences (Switzerland),
1029 8(12), 1–16. https://doi.org/10.3390/geosciences8120458
1030 Miller, R. O., & Kissel, D. E (2010) Comparison of Soil pH Methods on Soils of North America.
1031 Soil Science Society of America Journal, 74(1), 310–316.
1032 https://doi.org/10.2136/sssaj2008.0047
1033 Moreland, K., Tian, Z., Berhe, A. A., McFarlane, K. J., Hartsough, P., Hart, S. C., Bales, R., &
1034 O'Geen, A. T (2021) Deep in the Sierra Nevada critical zone: saprock represents a large
1035 terrestrial organic carbon stock. Environmental Research Letters, 16(12).
1036 https://doi.org/10.1088/1748-9326/ac3bfe

1037 Nave, L. E., Bowman, M., Gallo, A., Hatten, J. A., Heckman, K. A., Matosziuk, L., Possinger,
1038 A. R., SanClements, M., Sanderman, J., Strahm, B. D., Weiglein, T. L., & Swanston, C. W
1039 (2021) Patterns and predictors of soil organic carbon storage across a continental-scale
1040 network. Biogeochemistry, 156(1), 75–96. https://doi.org/10.1007/s10533-020-00745-9
1041 Nitzsche, K. N., Kalettka, T., Premke, K., Lischeid, G., Gessler, A., & Kayler, Z. E., 2017. Land-
1042 use and hydroperiod affect kettle hole sediment carbon and nitrogen biogeochemistry.
1043 Science of the Total Environment, 574, 46–56.
1044 https://doi.org/10.1016/j.scitotenv.2016.09.003
1045 Ogle, S. M., Breidt, F. J., Paustian, K., Biogeochemistry, S., Jan, N., Ogle, S. M., Breidt, F. J. A.
1046 Y., & Paustian, K (2005) Agricultural Management Impacts on Soil Organic Carbon
1047 Storage under Moist and Dry Climatic Conditions of Temperate and Tropical Regions
1048 Published by: Springer Stable URL: https://www.jstor.org/stable/20055160 REFERENCES
1049 Linked references are available. 72(1), 87–121. https://doi.org/10.1007/sl0533-004-0360-2
1050 Olson, K. R., & Gennadiev, A. N (2020) Dynamics of Soil Organic Carbon Storage and Erosion
1051 due to Land Use Change (Illinois, USA). Eurasian Soil Science, 53(4), 436–445.
1052 https://doi.org/10.1134/S1064229320040122
1053 Paul, E. A., Collins, H. P., & Leavitt, S. W (2001) Dynamics of resistant soil carbon of
1054 midwestern agricultural soils measured by naturally occurring 14C abundance. Geoderma,
1055 104(3–4), 239–256. https://doi.org/10.1016/S0016-7061(01)00083-0
1056 Paustian, K., Lehmann, J., Ogle, S., Reay, D., Robertson, G.P., Smith, P (2016) Climate- smart
1057 soils. Nature 532, 49–57. http://dx.doi.org/10.1038/nature17174.

1058 Paustian, K., Larson, E., Kent, J., Marx, E., & Swan, A (2019) Soil C Sequestration as a
1059 Biological Negative Emission Strategy. Frontiers in Climate, 1(October), 1–11.
1060 https://doi.org/10.3389/fclim.2019.00008
1061 Polain, K., Knox, O., Wilson, B., & Pereg, L (2020) Subsoil microbial diversity and stability in
1062 rotational cotton systems. Soil Systems, 4(3), 1–18.
1063 https://doi.org/10.3390/soilsystems4030044
1064 Pittman, J. J., Zhang, H., Schroder, J. L., & Payton, M. E (2005) Differences of phosphorus in
1065 Mehlich 3 extracts determined by colorimetric and spectroscopic methods. Communications
1066 in Soil Science and Plant Analysis, 36(11–12), 1641–1659. https://doi.org/10.1081/CSS-
1067 200059112
1068 Possinger, A. R., Weiglein, T. L., Bowman, M. M., Gallo, A. C., Hatten, J. A., Heckman, K. A.,
1069 Matosziuk, L. M., Nave, L. E., SanClements, M. D., Swanston, C. W., & Strahm, B. D
1070 (2021) Climate Effects on Subsoil Carbon Loss Mediated by Soil Chemistry. Environmental
1071 Science and Technology, 55(23), 16224–16235. https://doi.org/10.1021/acs.est.1c04909
1072 Rasmussen, C., Heckman, K., Wieder, W. R., Keiluweit, M., Lawrence, C. R., Berhe, A. A.,
1073 Blankinship, J. C., Crow, S. E., Druhan, J. L., Hicks Pries, C. E., Marin-Spiotta, E., Plante,
1074 A. F., Schädel, C., Schimel, J. P., Sierra, C. A., Thompson, A., & Wagai, R (2018) Beyond
1075 clay: towards an improved set of variables for predicting soil organic matter content.
1076 Biogeochemistry, 137(3), 297–306. https://doi.org/10.1007/s10533-018-0424-3
1077 Rasse, D. P., Mulder, J., Moni, C., & Chenu, C (2006) Carbon Turnover Kinetics with Depth in a
1078 French Loamy Soil. Soil Science Society of America Journal, 70(6), 2097–2105.
1079 https://doi.org/10.2136/sssaj2006.0056

Rasse, D. P., Rumpel, C., & Dignac, M. F (2005) Is soil carbon mostly root carbon? Mechanisms for specific stabilisation. Plant and Soil, 269(1–2), 341–356. https://doi.org/10.1007/s11104-004-0907-y

Reichstein, M., Bahn, M., Ciais, P., Frank, D., Mahecha, M. D., Seneviratne, S. I., Zscheischler, J., Beer, C., Buchmann, N., Frank, D. C., Papale, D., Rammig, A., Smith, P., Thonicke, K., Van Der Velde, M., Vicca, S., Walz, A., & Wattenbach, M (2013) Climate extremes and the carbon cycle. Nature, 500(7462), 287–295. https://doi.org/10.1038/nature12350

Romdhane, S., Spor, A., Banerjee, S., Breuil, M. C., Bru, D., Chabbi, A., Hallin, S., van der Heijden, M. G. A., Saghai, A., & Philippot, L (2022) Land-use intensification differentially affects bacterial, fungal and protist communities and decreases microbiome network complexity. Environmental Microbiomes, 17(1), 1–15. https://doi.org/10.1186/s40793-021-00396-9

Rowley, M. C., Grand, S., & Verrecchia, É. P (2018) Calcium-mediated stabilisation of soil organic carbon. Biogeochemistry, 137(1–2), 27–49. https://doi.org/10.1007/s10533-017-0410-1

Rumpel, C., & Kögel-Knabner, I (2011) Deep soil organic matter-a key but poorly understood component of terrestrial C cycle. Plant and Soil, 338(1), 143–158. https://doi.org/10.1007/s11104-010-0391-5

Sanderman, J., Hengl, T., & Fiske, G. J (2017) Soil carbon debt of 12,000 years of human land use. Proceedings of the National Academy of Sciences of the United States of America, 114(36), 9575–9580. https://doi.org/10.1073/pnas.1706103114

1101 Sanderman, J., Baldock, J. A., and Amundson, R (2008) Dissolved organic carbon chemistry and
1102 dynamics in contrasting forest and grassland soils, Biogeochemistry, 89, 181–198,
1103 https://doi.org/10.1007/s10533-008-9211-x
1104 Sanford, G. R., Jackson, R. D., Rui, Y., & Kucharik, C. J (2022) Land use-land cover gradient
1105 demonstrates the importance of perennial grasslands with intact soils for building soil carbon
1106 in the fertile Mollisols of the North Central US. Geoderma 418, 1-11.

1107 Salonen, A.-R., Soinne, H., Creamer, R., Lemola, R., Ruoho, N., Uhlgren, O., de Goede, R., &
1108 Heinonsalo, J (2023) Assessing the effect of arable management practices on carbon storage
1109 and fractions after 24 years in boreal conditions of Finland. Geoderma Regional, e00678.
1110 https://doi.org/10.1016/j.geodrs.2023.e00678

1111 Scheibe, A., Sierra, C. A., & Spohn, M (2023) Recently fixed carbon fuels microbial activity
1112 several meters below the soil surface. Biogeosciences 20, 827–838.
1113 https://doi.org/10.5194/bg-2022-199
1114 Schulte, E. E., & Eik, K (1988) Recommended sulfate-sulfur test. In recommended chemical soil
1115 test procedures for north central region. In W. C. Dahnke, (Ed.) Bulletin no. 499 (revised).
1116 (pp. 17–19). North Dakota Agriculture Experiment Station.
1117 Sherrod, L. A., Dunn, G., Peterson, G. A., & Kolberg, R. L (2002) Inorganic Carbon Analysis by
1118 Modified Pressure-Calcimeter Method. Soil Science Society of America Journal, 66(1),
1119 299–305. https://doi.org/10.2136/sssaj2002.2990
1120 Shimada, H., Wagai, R., Inoue, Y., Tamura, K., & Asano, M (2022) Millennium timescale
1121 carbon stability in an Andisol: How persistent are organo-metal complexes? Geoderma,
1122 417, 115820. https://doi.org/10.1016/j.geoderma.2022.115820

Sierra, C. A., Ahrens, B., Bolinder, M. A., Braakhekke, M. C., von Fromm, S., Kätterer, T., Luo, Z., Parvin, N., & Wang, G (2024). Carbon sequestration in the subsoil and the time required to stabilize carbon for climate change mitigation. Global Change Biology, 30(1), 1–26. https://doi.org/10.1111/gcb.17153

Skadell, L. E., Schneider, F., Gocke, M. I., Guigue, J., Amelung, W., Bauke, S. L., Hobley, E. U., Barkusky, D., Honermeier, B., Siebert, S., Sommer, M., Vaziritabar, Y., & Don, A (2023) Agriculture, Ecosystems and Environment Twenty percent of agricultural management effects on organic carbon stocks occur in subsoils – Results of ten long-term experiments. 356.

Slessarev, E. W., Nuccio, E. E., McFarlane, K. J., Ramon, C. E., Saha, M., Firestone, M. K., & Pett-Ridge, J (2020) Quantifying the effects of switchgrass (Panicum virgatum) on deep organic C stocks using natural abundance ^{14}C in three marginal soils. GCB Bioenergy, 12(10), 834–847. https://doi.org/10.1111/gcbb.12729

Soil Survey Staff (2014) Soil Survey Field and Laboratory Methods Manual. In Soil Survey Investigations Report No. 51, Version 2.0; Burt, R., Ed.; U.S. Department of Agriculture, Natural Resources Conservation Service.

Soil Survey Staff (2022) Keys to Soil Taxonomy, Thirteenth Edition. United States Department of Agriculture Natural Resources Conservation Service, 1–410. http://www.nrcs.usda.gov/Internet/FSE_DOCUMENTS/nrcs142p2_051546.pdf

Sokol, N. W., Slessarev, E., Marschmann, G. L., Nicolas, A., Blazewicz, S. J., Brodie, E. L., Firestone, M. K., Foley, M. M., Hestrin, R., Hungate, B. A., Koch, B. J., Stone, B. W., Sullivan, M. B., Zablocki, O., Trubl, G., McFarlane, K., Stuart, R., Nuccio, E., Weber, P.,

Pett-Ridge, J (2022) Life and death in the soil microbiome: how ecological processes influence biogeochemistry. Nature Reviews Microbiology, 20(7), 415–430. https://doi.org/10.1038/s41579-022-00695-z

Stuiver M, & Polach, H.A (1977). Discussion: reporting of ^{14}C data. Radiocarbon 19:355–363. https://doi.org/10.1017/ S0033822200003672

Tautges, N. E., Chiartas, J. L., Gaudin, A. C. M., O'Geen, A. T., Herrera, I., & Scow, K. M (2019) Deep soil inventories reveal that impacts of cover crops and compost on soil carbon sequestration differ in surface and subsurface soils. Global Change Biology, 25(11), 3753–3766. https://doi.org/10.1111/gcb.14762

United States Department of Agriculture, Natural Resources Conservation Service (2022) Land resource regions and major land resource areas of the United States, the Caribbean, and the Pacific Basin. U.S. Department of Agriculture, Agriculture Handbook 296.

Upton, R. N., Checinska Sielaff, A., Hofmockel, K. S., Xu, X., Polley, H. W., & Wilsey, B. J (2020) Soil depth and grassland origin cooperatively shape microbial community co-occurrence and function. Ecosphere, 11(1). https://doi.org/10.1002/ecs2.2973

Van Der Voort, T. S., Mannu, U., Hagedorn, F., McIntyre, C., Walthert, L., Schleppi, P., Haghipour, N., & Eglinton, T. I (2019) Dynamics of deep soil carbon - Insights from 14C time series across a climatic gradient. Biogeosciences, 16(16), 3233–3246. https://doi.org/10.5194/bg-16-3233-2019

Viscarra Rossel, R. A., Lee, J., Behrens, T., Luo, Z., Baldock, J., & Richards, A (2019) Continental-scale soil carbon composition and vulnerability modulated by regional

environmental controls. Nature Geoscience, 12(7), 547–552. https://doi.org/10.1038/s41561-019-0373-z

Vogel J.S., Southon J.R., Nelson D.E (1987) Catalyst and binder effects in the use of filamentous graphite for AMS. Nuclear Instruments & Methods in Physics Research, Sect B 29:50–56. https://doi. org/10.1016/0168-583X (87)90202-3

Vormstein, S., Kaiser, M., Piepho, H. P., & Ludwig, B (2020) Aggregate formation and organo-mineral association affect characteristics of soil organic matter across soil horizons and parent materials in temperate broadleaf forest. Biogeochemistry, 148(2), 169–189. https://doi.org/10.1007/s10533-020-00652-z

Wang, B., An, S., Liang, C., Liu, Y., & Kuzyakov, Y (2021) Microbial necromass as the source of soil organic carbon in global ecosystems. Soil Biology and Biochemistry, 162, 108422. https://doi.org/10.1016/j.soilbio.2021.108422

Wang, S., Gao, X., Yang, M., Zhang, L., Wang, X., Wu, P., & Zhao, X (2022) The efficiency of organic C sequestration in deep soils is enhanced by drier climates. Geoderma, 415(26), 115774. https://doi.org/10.1016/j.geoderma.2022.115774

Wendt, J. W., & Hauser, S (2013) An equivalent soil mass procedure for monitoring soil organic carbon in multiple soil layers. European Journal of Soil Science, 64(1), 58–65. https://doi.org/10.1111/ejss.12002

Wiesmeier, M., Urbanski, L., Hobley, E., Lang, B., von Lützow, M., Marin-Spiotta, E., van Wesemael, B., Rabot, E., Ließ, M., Garcia-Franco, N., Wollschläger, U., Vogel, H. J., & Kögel-Knabner, I (2019) Soil organic carbon storage as a key function of soils - A review of drivers and indicators at various scales. Geoderma, 333, 149–162. https://doi.org/10.1016/j.geoderma.2018.07.026

1189 Wiesmeier, M., Hübner, R., Barthold, F., Spörlein, P., Geuß, U., Hangen, E., Reischl, A.,
1190 Schilling, B., von Lützow, M., & Kögel-Knabner, I (2013) Amount, distribution and driving
1191 factors of soil organic carbon and nitrogen in cropland and grassland soils of southeast
1192 Germany (Bavaria). Agriculture, Ecosystems and Environment, 176, 39–52.
1193 https://doi.org/10.1016/j.agee.2013.05.012
1194 Wood, S. A., & Bowman, M (2021) Large-scale farmer-led experiment demonstrates positive
1195 impact of cover crops on multiple soil health indicators. Nature Food, 2(2), 97–103.
1196 https://doi.org/10.1038/s43016-021-00222-y
1197 Xiao, J., Wang, X., Zhao, Y., Li, J., Tang, J., Wang, K., & Hao, Z (2023) Soil organic carbon
1198 stability of vegetation restoration during 11 - year - old grassland succession. Journal of
1199 Soils and Sediments, 0123456789. https://doi.org/10.1007/s11368-023-03497-9
1200 Yost, J. L., & Hartemink, A. E (2020) How deep is the soil studied – an analysis of four soil
1201 science journals. Plant and Soil, 452(1–2), 5–18. https://doi.org/10.1007/s11104-020-
1202 04550-z
1203 Yu, W., Weintraub, S. R., & Hall, S. J (2021) Climatic and geochemical controls on soil carbon
1204 at the continental scale: Interactions and thresholds. Global Biogeochemical Cycles, 35(3),
1205 e2020GB006781. https://doi.org/10.1029/2020GB006781
1206

Figures

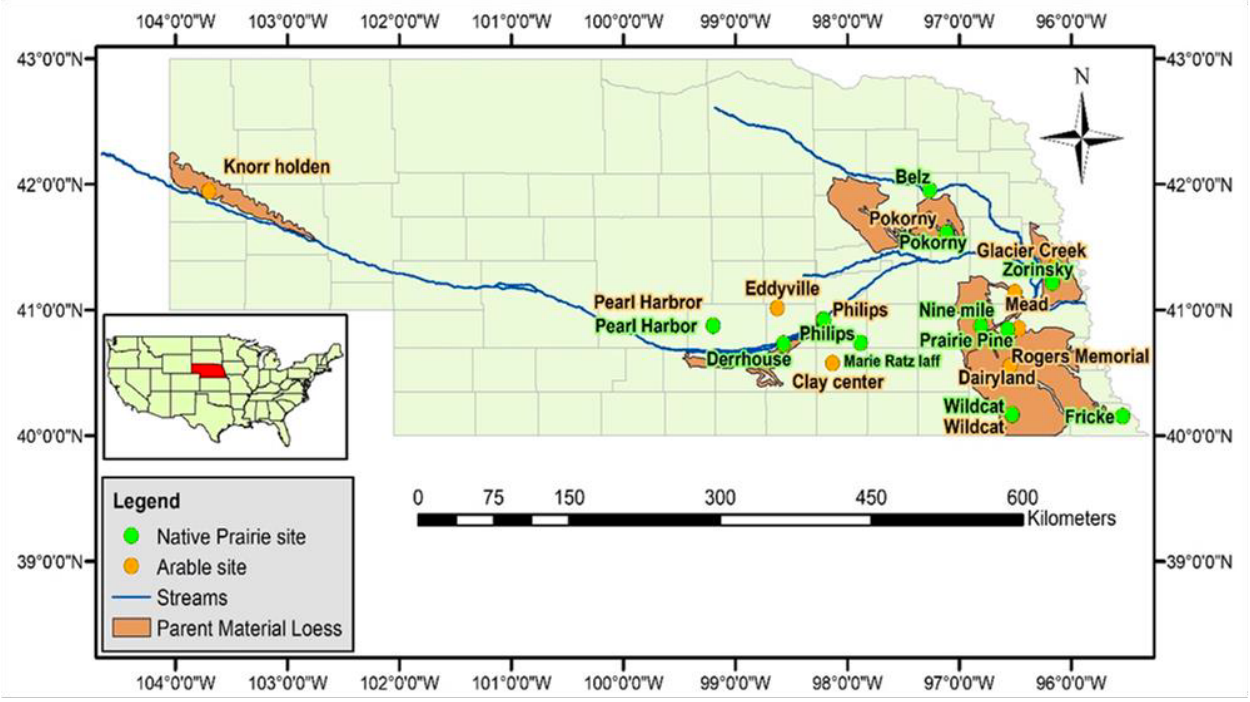

Fig. 1 Map showing the long-term (> 40 years) arable (orange circle) and the native prairie (green circle) sites in Nebraska

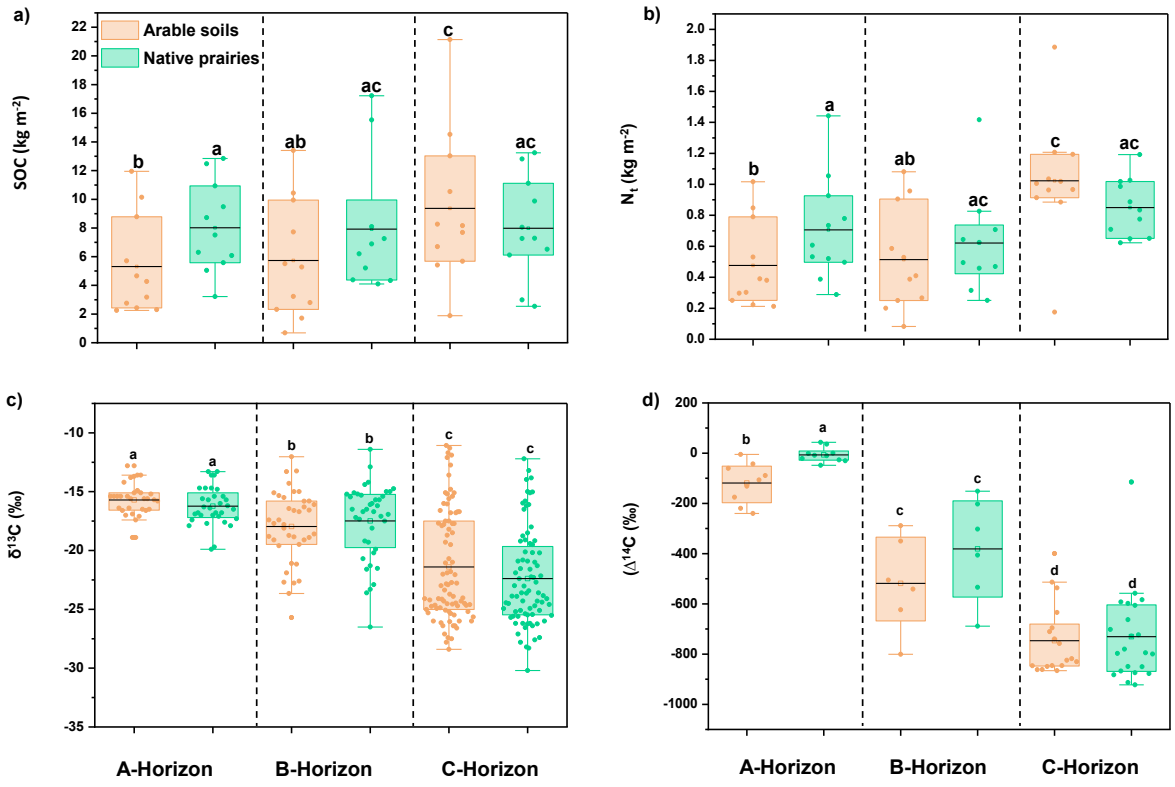

Fig. 2 Mean soil organic carbon (SOC) and total nitrogen (N) stocks (kg m) (a-b) and δ C and selected Δ C of SOC (c-d) compared between arable and native prairie sites across A, B, and C horizons to a depth of 3 m (300 cm). For SOC and total N stocks, the box plots display site-specific mean values (represented by the scattered orange and green dots) derived from three replicated cores per site, with a total of 11 sites for each land use type. For the δ C and Δ C of SOC, the orange and green dots represent the total number of samples utilized for analysis from all A, B, and C horizons in each land use type. Different letters indicate significant differences ($p \leq 0.05$) between land uses for each horizon.

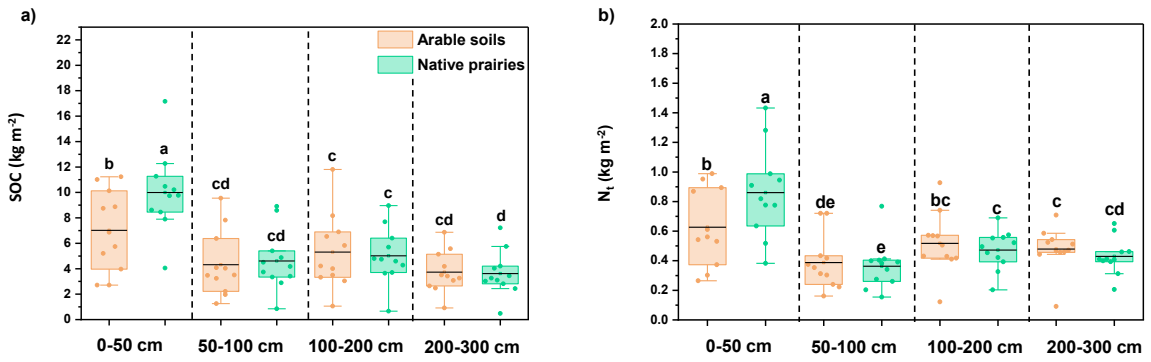

Fig. 3 Mean soil organic carbon (SOC) and total nitrogen (N) stocks (kg m) compared between arable and native prairie sites across 0–50, 50–100, 100–200, and 200–300 cm depth increments. The box plots display site-specific mean values (represented by the scattered orange and green dots) derived from three replicated cores per site, with a total of 11 sites for each land use type. Different letters denote significant differences ($p \leq 0.05$) between land uses for each depth increment.

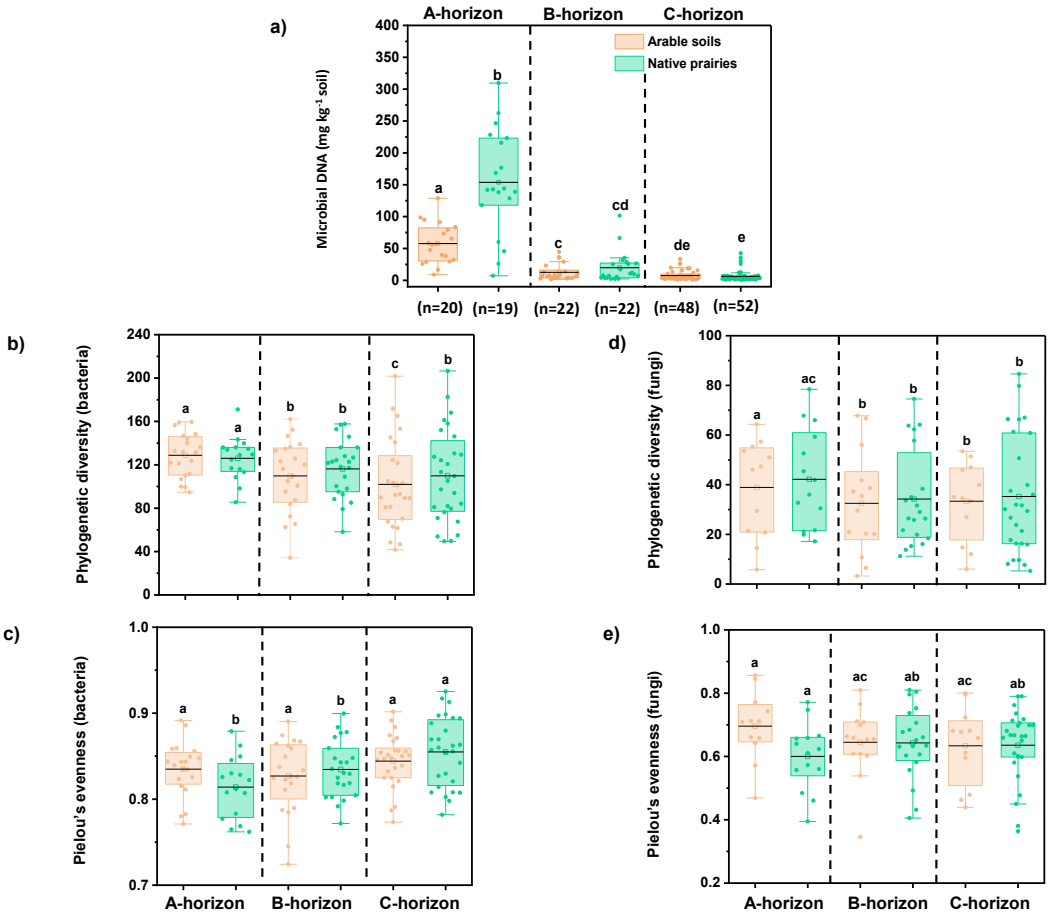

Fig. 4 Comparison of mean soil microbial DNA concentrations (a) and Faith's phylogenetic diversity and evenness (Pielou's evenness) of soil bacteria (b and c) and fungi (d and e) communities across A, B, and C horizons in arable and native prairie sites. The box plots depict the total number of samples (n) utilized for analysis from all horizons in both land use types (represented by scattered orange and green dots). Significant differences between land uses at $p \leq 0.05$ for each horizon are indicated by different letters.

1242 # Tables

Table 1. Range, mean, and standard error of soil properties, including pH, bulk density (BD), percentage of sand, silt, and clay content, soil organic carbon (SOC), and total nitrogen (Nt) concentrations across arable and native prairie sites for A, B, and C horizons. Significant differences between land uses at $p \leq 0.05$ for each horizon are denoted by different letters. Given variations in horizon thickness across arable and native prairie sites, the upper (minimum) and lower (maximum) depth ranges for individual horizons are provided. For example, 0-12-38 cm indicates that the upper depth ranged from 0 to 12 cm, while the lower depth ranged from 0 to 38 cm.

Land use	Horizon	Depth ranges (cm) (upper and lower)	Soil pH	SOC (g kg^{-1})	N_t (g kg^{-1})	BD (g cm^{-3})	Sand (%)	Silt (%)	Clay (%)
Arable	A	0-12-38	5.3-8.0 6.6 ± 0.1 a n=33	5.5-22 13 ± 0.8 a n=33	0.5-1.8 1.2 ± 0.1 a n=33	0.8-1.5 1.2 ± 0.03 a n=33	18-63 39 ± 2.3 a n=33	10-56 36 ± 2.0 a n=33	13-34 23 ± 0.9 a n=33
Native prairie	A	0-17-38	5.6-7.3 6.3 ± 0.1 a n=33	7.0-36 22 ± 1.2 b n=33	0.6-3.4 1.9 ± 0.1 b n=33	0.9-1.4 1.1 ± 0.02 a n=33	18-92 44 ± 2.9 a n=33	0-60 36 ± 2.4 a n=33	2.0-34 19 ± 1.0 a n=33
Arable	B	12-28-170	6.0-8.7 7.5 ± 0.1 cd n=40	0.7-18 6.1 ± 0.6 c n=40	0.2-1.8 0.6 ± 0.1 c n=40	0.8-1.9 1.4 ± 0.04 c n=40	13-86 39 ± 2.1 ac n=40	8-60 37 ± 1.6 c n=40	5-33 21 ± 1.1 c n=40
Native Prairie	B	17-28-176	5.8-8.6 7.1 ± 0.1 cd n=41	1.2-18 6.5 ± 0.6 c n=41	0.1-1.5 0.5 ± 0.04 c n=41	1.1-1.9 1.5 ± 0.03 c n=41	18-62 34 ± 1.6 c n=41	14-66 43 ± 1.8 ac n=41	11-34 22 ± 0.9 c n=41
Arable	C	28-170-300	6.7-8.8 8.0 ± 0.1 d n=87	0.5-10 2.5 ± 0.2 d n=87	0.04-0.9 0.3 ± 0.01 d n=87	1.2-2.3 1.8 ± 0.03 d n=87	11-88 40 ± 1.8 ad n=87	8.0-74 42 ± 1.5 ac n=87	1.3-38 17 ± 0.9 d n=87
Native Prairie	C	28-176-300	6.1-8.6 7.8 ± 0.1d n=80	0.2-5.9 2.4 ± 0.2 d n=80	0.04-0.7 0.3 ± 0.01 d n=80	1.1-2.3 1.7 ± 0.03 d n=80	8.5-98 45 ± 2.4 ad n=80	0-72 38 ± 2 ac n=80	2-33 16 ± 0.9 d n=80

n: total number of samples utilized for analysis from all A, B, and C horizons in arable and native prairie sites.

1243

1244

Table 2. Range, mean, and standard error of exchangeable calcium (Ca), magnesium (Mg), potassium (K), and cation exchange capacity (CEC) across arable and native prairie sites for A, B, and C horizons. Significant differences between land uses at $p \leq 0.05$ for each horizon are indicated by different letters.

Land use	Horizon	Depth ranges (cm) (upper and lower)	Ca (mg kg^{-1})	Mg (mg kg^{-1})	K (mg kg^{-1})	CEC (cmol kg^{-1})
Arable	A	0-12-38	1881-4548 3083 ± 106 a n=33	274-957 604 ± 29 a n=33	198-1093 427 ± 34 a n=33	13-31 22 ± 0.7 a n=33
Native prairie	A	0-17-38	723-3286 2475 ± 103 a n=33	108-822 514 ± 28 a n=33	93-634 361 ± 28 a n=33	5.5-27 20 ± 0.8 a n=33
Arable	B	12-28-170	1999-6040 3901 ± 140 c n=40	291-1377 740 ± 38 b n=40	163-775 338 ± 29 c n=40	13-35 26 ± 0.7 b n=40
Native Prairie	B	17-28-176	2255-5529 3292 ± 118 c n=41	484-1030 789 ± 23 b n=41	91-679 292 ± 24 cd n=41	16-33 24 ± 0.6 b n=41
Arable	C	28-170-300	2061-5495 3612 ± 90 c n=87	222-1797 720 ± 30 c n=87	129-922 389 ± 24 ac n=87	13-35 25 ± 0.5 b n=87
Native Prairie	C	28-176-300	259-5446 3178 ± 148 c n=80	52-1133 639 ± 27 c n=80	42-812 281 ± 21 ac n=80	2.0-33 22 ± 0.8 b n=80

n: total number of samples utilized for analysis from all A, B, and C horizons in arable and native prairie sites.

1245

Table 3. Range, mean, and standard error of reactive Fe and Al oxides phases across arable and native prairie sites for A, B, and C horizons. Significant differences between land uses at $p \leq 0.05$ for each horizon are indicated by different letters.

Land use	Horizon	Depth ranges (cm) (upper and lower)	Al_{AO} (mg kg^{-1})	Fe_{AO} (mg kg^{-1})	Al_{DCB} (mg kg^{-1})	Fe_{DCB} (mg kg^{-1})
Arable	A	0-12-38	193-1093 694 ± 36 a n=33	125-1962 859 ± 79 a n=33	147-974 468 ± 39 a n=33	706-15933 3802 ± 572 a n=33
Native prairie	A	0-17-38	150-1296 689 ± 57 a n=33	138-1534 833 ± 69 a n=33	103-2196 506 ± 69 a n=33	359-8066 2760 ± 342 a n=33
Arable	B	12-28-170	279-954 631 ± 25 a n=40	42-1643 739 ± 72 a n=40	93-900 349 ± 34 b n=40	572-7582 2496 ± 307 a n=40
Native Prairie	B	17-28-176	320-1282 717 ± 42 a n=41	253-1791 905 ± 66 a n=41	48-2673 551 ± 91 b n=41	274-10300 3071 ± 366 a n=41
Arable	C	28-170-300	178-729 438 ± 14 b n=87	56-2711 691 ± 52 b n=87	58-615 216 ± 14 c n=87	375-10678 3112 ± 284 a n=87
Native Prairie	C	28-176-300	34-1005 402 ± 19 b n=80	35-2996 676 ± 67 b n=80	31-1826 242 ± 26 c n=80	146-9683 3106 ± 291 a n=80

n: total number of samples utilized for analysis from all A, B, and C horizons in arable and native prairie sites.

Al_{AO}: ammonium oxalate extractable Aluminum, Fe_{AO}: ammonium oxalate extractable iron, Al_{DCB}: dithionite citrate bicarbonate extractable Aluminum; Fe_{DCB}: dithionite citrate bicarbonate extractable iron, n: total number of samples from all A, B, and C horizons in arable and native prairie sites.

1246

Table 4. Summary of range, mean, standard error, and sample size (n) (number of measurements per horizon and land use type) for $\delta^{13}C$ and $\Delta^{14}C$ data of bulk soil organic carbon across A, B, and C horizons in arable and native prairie soils, along with corresponding radiocarbon ages for reference. Different letters denote significant differences between land uses at $p \leq 0.05$ for each horizon. BP signifies "before present."

Land use				
		$\delta^{13}C$ (‰)		
	Horizons	A	B	C
Arable		-12.8 to -21.6 -15.8 ± 0.3 a n=33	-12.0 to -25.7 -17.9 ± 0.5 b n=39	-11.0 to -28.4 -21.4 ± 0.4 c n=87
Native prairie		-13.3 to -19.9 -16.2 ± 0.2 a n=33	-11.4 to -26.5 -17.3 ± 0.5 b n=41	-12.2 to -30.2 -22.3 ± 0.4 c n=80
		$\Delta^{14}C$ (‰) (^{14}C age in years BP)		
	Horizons	A	B	C
Arable		-5 to -240 -118 ± 26 b (285 - 2135 yrs.) n= 9	-288 to -800 -518 ± 75 c (2665 - 12890 yrs.) n=6	-399 to -865 -746 ± 33 d (4030 - 16060 yrs.) n=18
Native prairie		-48 to 43 -7 ± 8 a (105 - 330 yrs.) n=10	-151 to -688 -380 ± 83 c (1250 - 9310 yrs.) n=6	-114 to -922 -730 ± 38 d (910 - 20460 yrs.) n=22

1247

1248

Supplementary Material

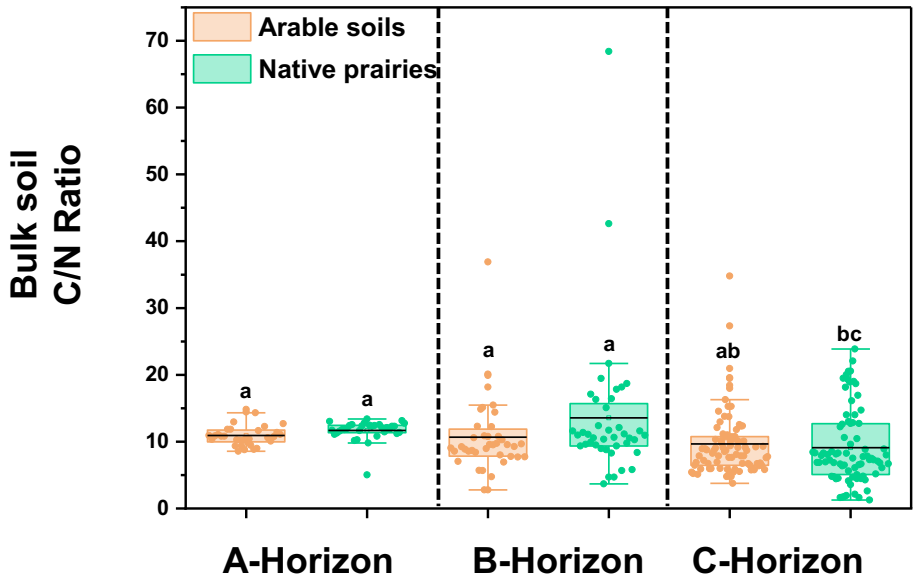

Figure S1. Mean soil carbon to nitrogen ratio (C/N) of bulk soil for arable (n = 11) and native prairie (n = 11) soils across A, B, and C horizons. The orange and green dots on the box plot represent individual data points for each horizon. Means with different letters indicate a significant difference between land uses at $p \leq 0.05$.

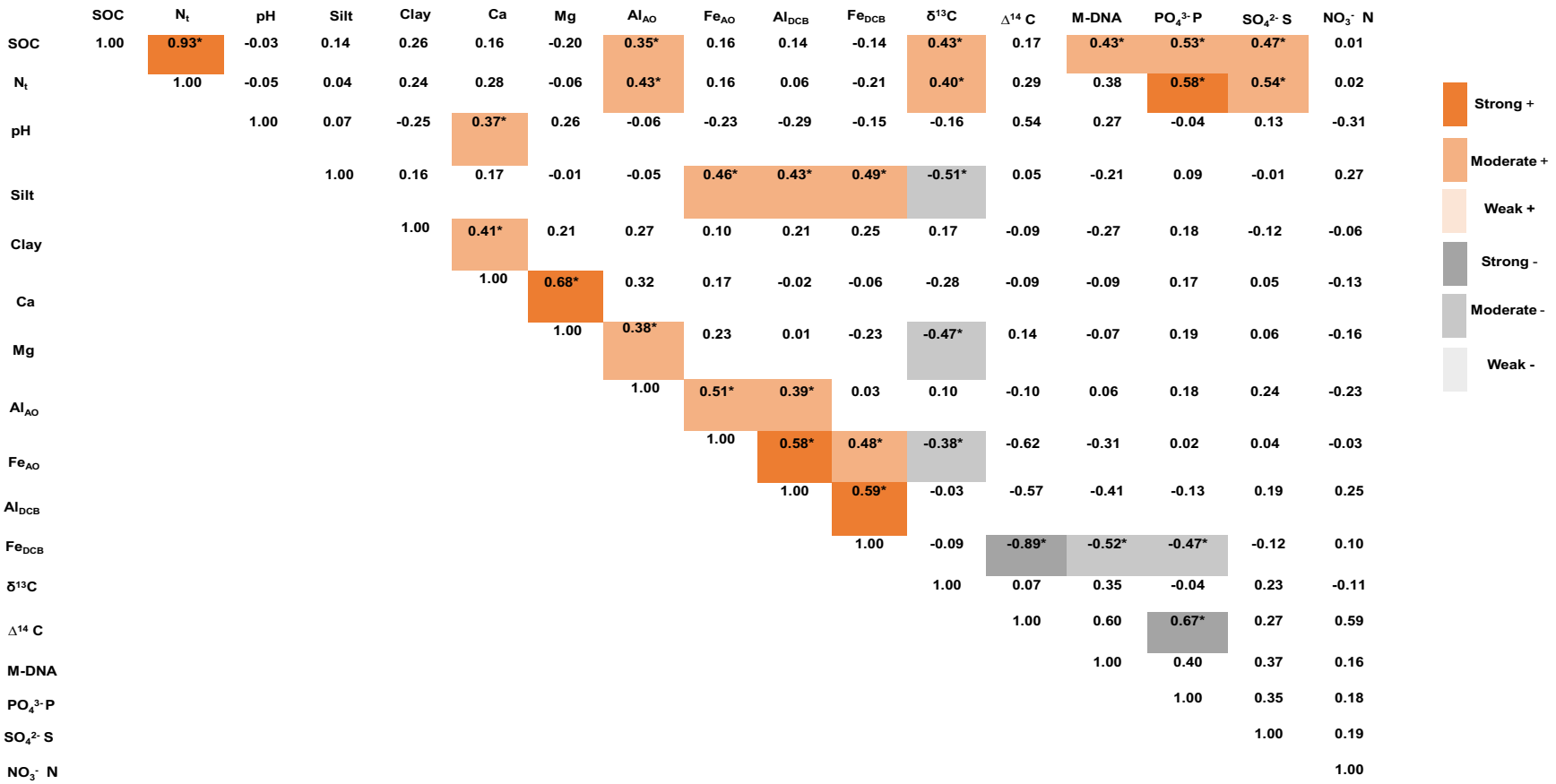

Figure S2a. Correlations between soil organic carbon (SOC) characteristics and soil physical, chemical, and biological properties in the A horizon of sites under arable land use. The symbol * indicates a significant correlation at $p \leq 0.05$. Abbreviations: SOC: soil organic carbon content, N_t: soil total nitrogen content, M-DNA: microbial DNA concentration, Ca: exchangeable cation, Mg: exchangeable magnesium, Al_{AO}: ammonium oxalate extractable Aluminum, Fe_{AO}: ammonium oxalate extractable iron, Al_{DCB}: dithionite citrate bicarbonate extractable Aluminum; Fe_{DCB}: dithionite citrate bicarbonate extractable iron, NO_3^- N: nitrate-nitrogen, PO_4^{3-}: phosphate-phosphorous, SO_4^{2-}: sulphate-Sulphur. Strong positive ($r > 0.5$), moderate positive ($0.3 \leq r \leq 0.5$), weak positive ($0 \leq r \leq 0.3$); strong negative ($r < -0.5$), moderate negative ($-0.3 \geq r \geq -0.5$), weak negative ($r \leq 0$ to -0.3).

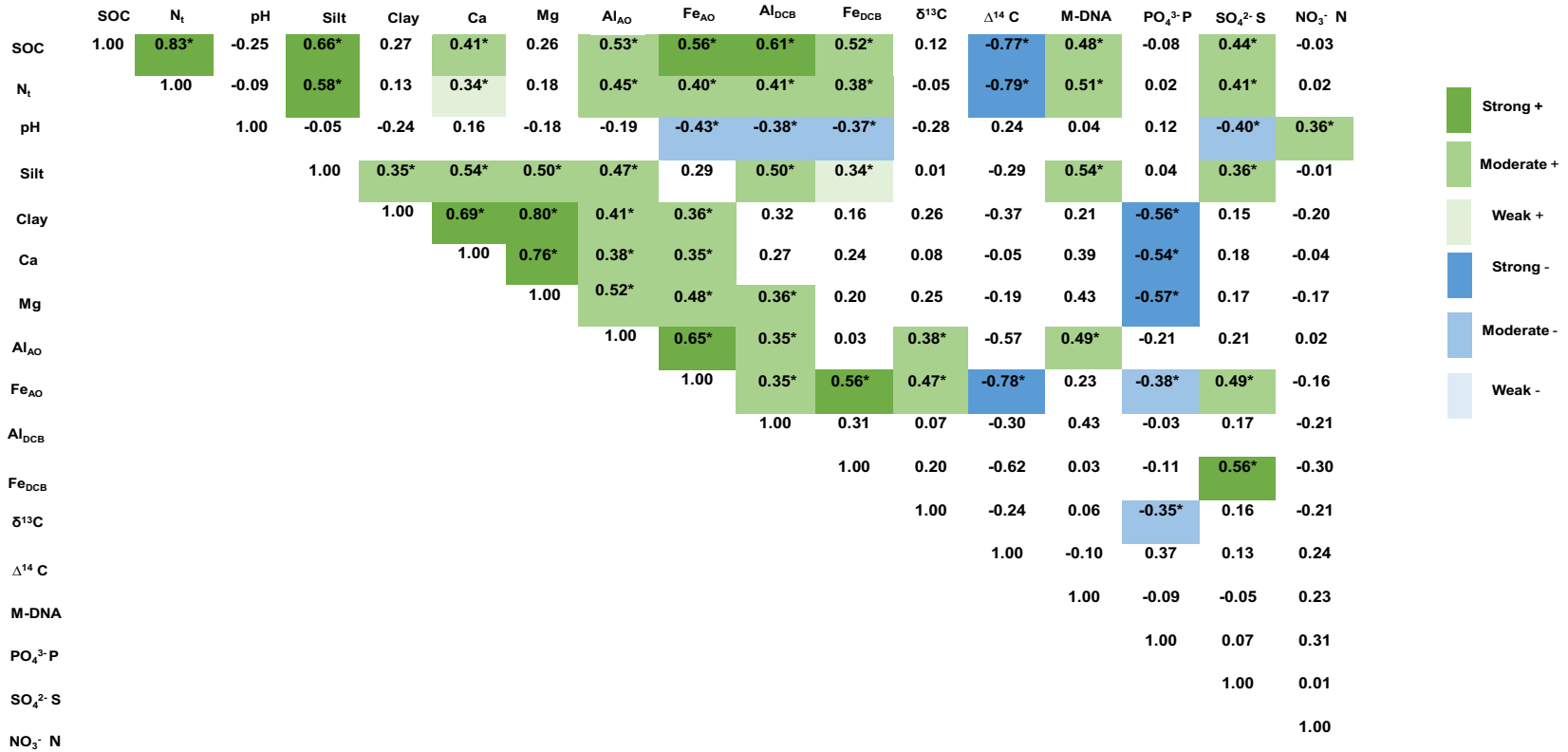

Figure S2b. Correlations between soil organic carbon (SOC) characteristics and soil physical, chemical, and biological properties in the A horizon of sites under native prairie land use. The symbol * indicates a significant correlation at $p \leq 0.05$. Abbreviations: SOC: soil organic carbon content, N_t: soil total nitrogen content, M-DNA: microbial DNA concentration, Ca: exchangeable cation, Mg: exchangeable magnesium, Al_{AO}: ammonium oxalate extractable Aluminum, Fe_{AO}: ammonium oxalate extractable iron, Al_{DCB}: dithionite citrate bicarbonate extractable Aluminum; Fe_{DCB}: dithionite citrate bicarbonate extractable iron, NO_3^- N: nitrate-nitrogen, PO_4^{3-}: phosphate-phosphorous, SO_4^{2-}: sulphate-Sulphur. Strong positive ($r > 0.5$), moderate positive ($0.3 \leq r \leq 0.5$), weak positive ($0 \leq r \leq 0.3$); strong negative ($r < -0.5$), moderate negative ($-0.3 \geq r \geq -0.5$), weak negative ($r \leq 0$ to -0.3).

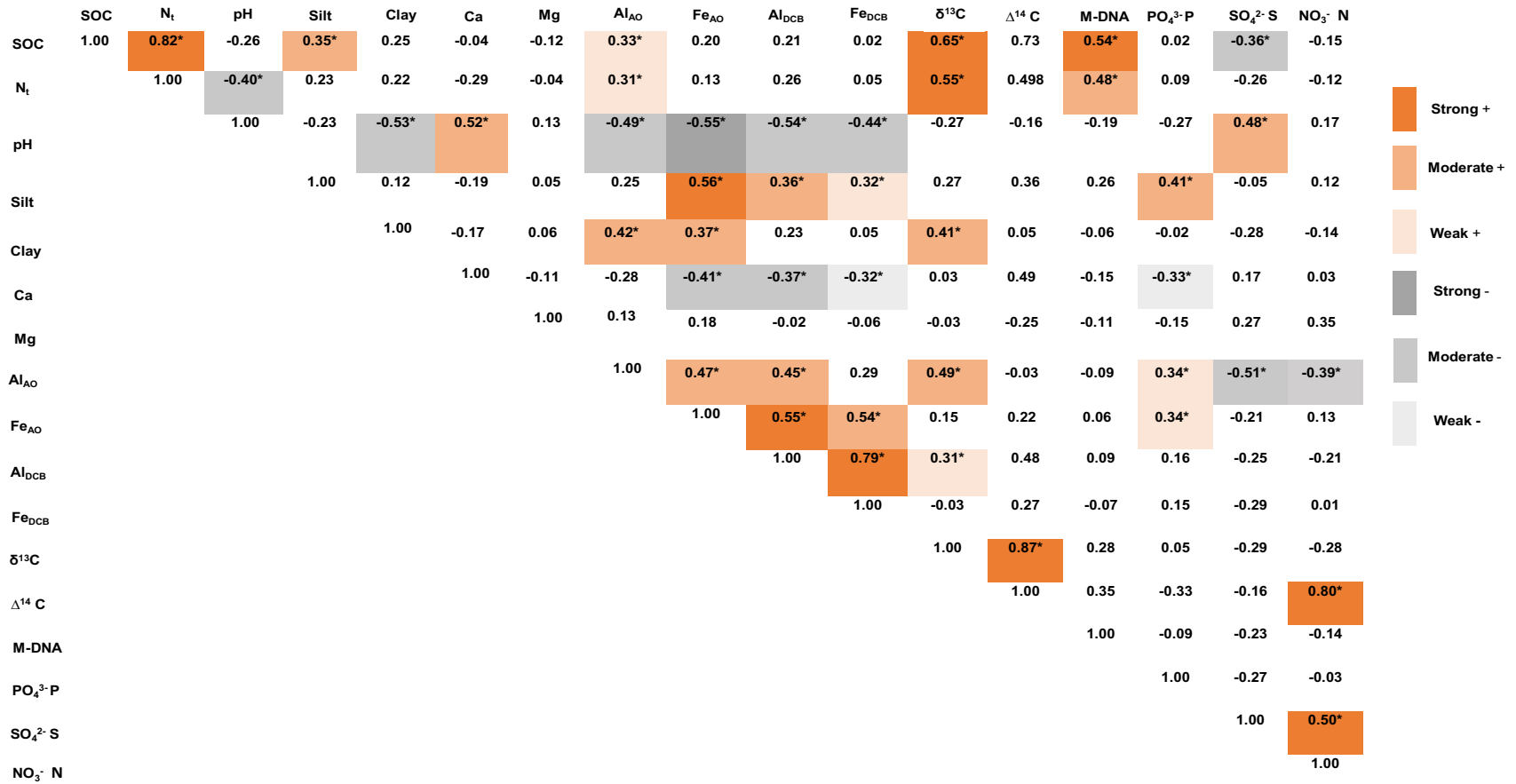

Figure S2c. Correlations between soil organic carbon (SOC) characteristics and soil physical, chemical, and biological properties in the B horizon of sites under arable land use. The symbol * indicates a significant correlation at $p \leq 0.05$. Abbreviations: SOC: soil organic carbon content, N_t: soil total nitrogen content, M-DNA: microbial DNA concentration, Ca: exchangeable cation, Mg: exchangeable magnesium, Al_{AO}: ammonium oxalate extractable Aluminum, Fe_{AO}: ammonium oxalate extractable iron, Al_{DCB}: dithionite citrate bicarbonate extractable Aluminum; Fe_{DCB}: dithionite citrate bicarbonate extractable iron, NO_3^- N: nitrate-nitrogen, PO_4^{3-}: phosphate-phosphorous, SO_4^{2-}: sulphate-Sulphur. Strong positive ($r > 0.5$), moderate positive ($0.3 \leq r \leq 0.5$), weak positive ($0 \leq r \leq 0.3$); strong negative ($r < -0.5$), moderate negative ($-0.3 \geq r \geq -0.5$), weak negative ($r \leq 0$ to -0.3).

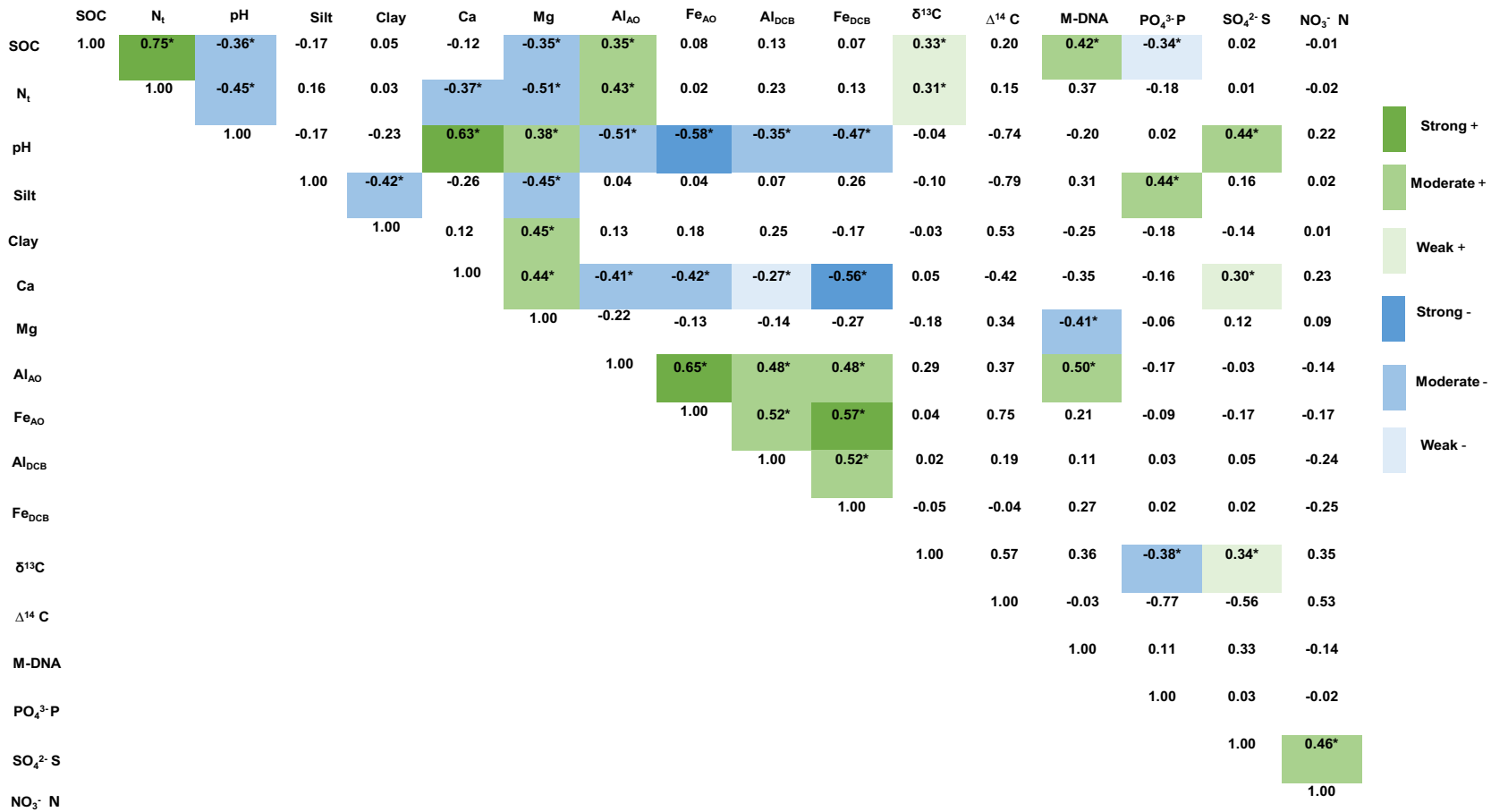

Figure S2d. Correlations between soil organic carbon (SOC) characteristics and soil physical, chemical, and biological properties in the B horizon of sites under native prairie land use. The symbol * indicates a significant correlation at $p \leq 0.05$. Abbreviations: SOC: soil organic carbon content, N_t: soil total nitrogen content, M-DNA: microbial DNA concentration, Ca: exchangeable cation, Mg: exchangeable magnesium, Al_{AO}: ammonium oxalate extractable Aluminum, Fe_{AO}: ammonium oxalate extractable iron, Al_{DCB}: dithionite citrate bicarbonate extractable Aluminum; Fe_{DCB}: dithionite citrate bicarbonate extractable iron, NO_3^- N: nitrate-nitrogen, PO_4^{3-}: phosphate-phosphorous, SO_4^{2-}: sulphate-Sulphur. Strong positive ($r > 0.5$), moderate positive ($0.3 \leq r \leq 0.5$), weak positive ($0 \leq r \leq 0.3$); strong negative ($r < -0.5$), moderate negative ($-0.3 \geq r \geq -0.5$), weak negative ($r \leq 0$ to -0.3).

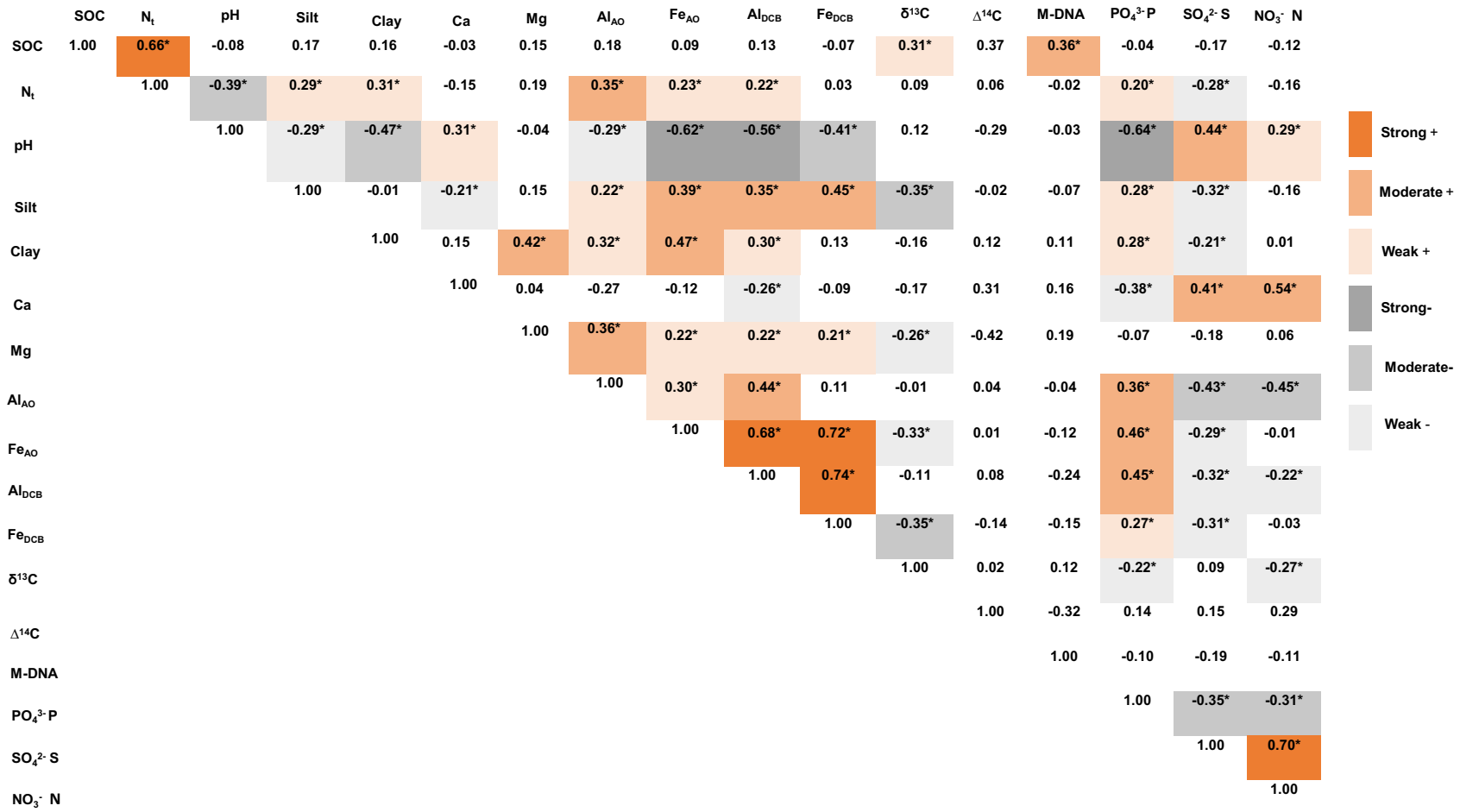

Figure S2e. Correlations between soil organic carbon (SOC) characteristics and soil physical, chemical, and biological properties in the C horizon of sites under arable land use. The symbol * indicates a significant correlation at $p \leq 0.05$. Abbreviations: SOC: soil organic carbon content, N_t: soil total nitrogen content, M-DNA: microbial DNA concentration, Ca: exchangeable cation, Mg: exchangeable magnesium, Al_{AO}: ammonium oxalate extractable Aluminum, Fe_{AO}: ammonium oxalate extractable iron, Al_{DCB}: dithionite citrate bicarbonate extractable Aluminum; Fe_{DCB}: dithionite citrate bicarbonate extractable iron, NO_3^- N: nitrate-nitrogen, PO_4^{3-}: phosphate-phosphorous, SO_4^{2-}: sulphate-Sulphur. Strong positive ($r > 0.5$), moderate positive ($0.3 \leq r \leq 0.5$), weak positive ($0 \leq r \leq 0.3$); strong negative ($r < -0.5$), moderate negative ($-0.3 \geq r \geq -0.5$), weak negative ($r \leq 0$ to -0.3).

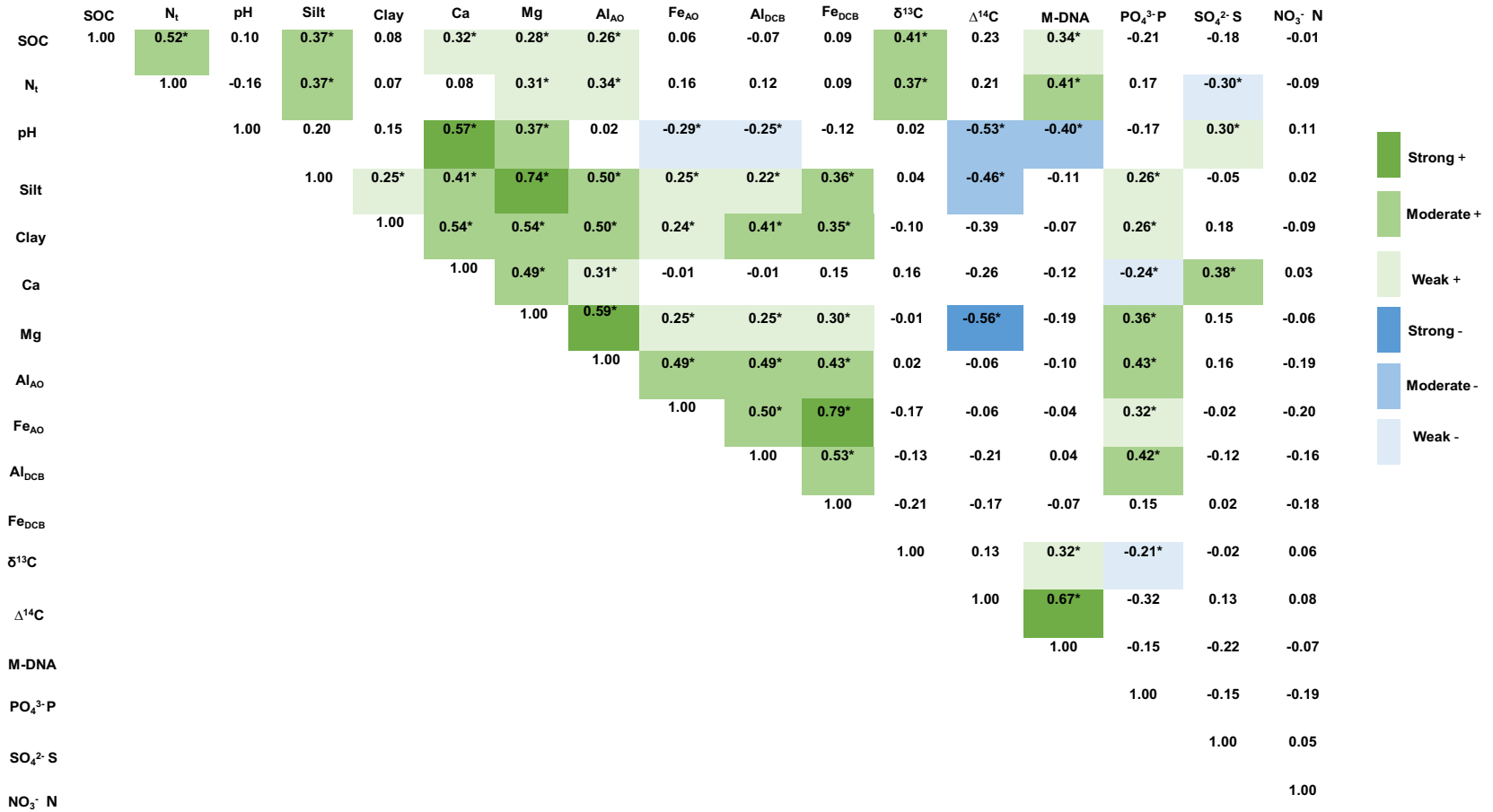

Figure S2f. Correlations between soil organic carbon (SOC) characteristics and soil physical, chemical, and biological properties in the C horizon of sites under native prairie land use. The symbol * indicates a significant correlation at $p \leq 0.05$. Abbreviations: SOC: soil organic carbon content, N_t: soil total nitrogen content, M-DNA: microbial DNA concentration, Ca: exchangeable cation, Mg: exchangeable magnesium, Al_{AO}: ammonium oxalate extractable Aluminum, Fe_{AO}: ammonium oxalate extractable iron, Al_{DCB}: dithionite citrate bicarbonate extractable Aluminum; Fe_{DCB}: dithionite citrate bicarbonate extractable iron, NO_3^- N: nitrate-nitrogen, PO_4^{3-}: phosphate-phosphorous, SO_4^{2-}: sulphate-Sulphur. Strong positive ($r > 0.5$), moderate positive ($0.3 \leq r \leq 0.5$), weak positive ($0 \leq r \leq 0.3$); strong negative ($r < -0.5$), moderate negative ($-0.3 \geq r \geq -0.5$), weak negative ($r \leq 0$ to -0.3).

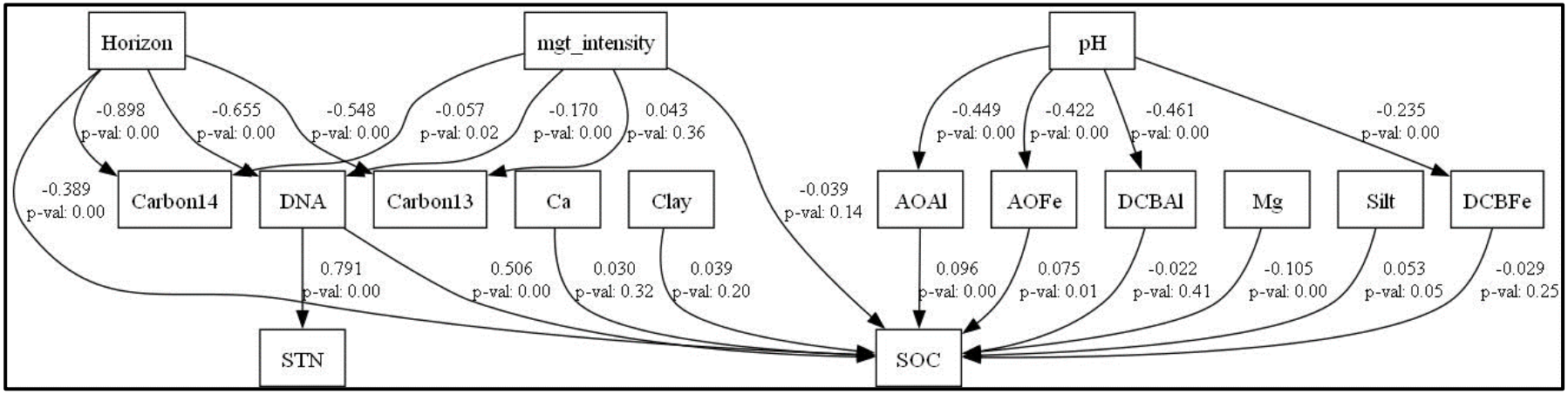

Figure S3. Structural equation model measuring the impact of management intensity and soil horizon on SOC and other soil biogeochemical properties and how these variables interact with each other to produce the overall effect on SOC storage. Boxes indicate variables. An arrow represents a causal relationship ($P < 0.05$). The arrow direction indicates the direction of effect. Numbers beside arrows are standardized path coefficients. GFI = 0.568, and CFI = 0.580. All the data was log-transformed for normality. Abbreviations: mgt_intensity: management intensity, carbon 14; $\Delta^{14}C$, carbon 13; $\delta^{13}C$, DNA: microbial DNA.

Table S1. Site names, locations, climatic conditions, vegetation, and management practices, parent material, soil type, and dominant soil orders in arable and native prairie sites studied to evaluate the impact of land use on soil organic carbon (SOC) stocks. Abbreviations: MLRA = Major land resource areas of the United States, MAT = Average annual temperature (range), MAP = Average annual precipitation (range).

Sites name	Location	Latitude (dec. °N)	Longitude (dec. °W)	MLRA	MAT (℃)	MAP (mm)	Vegetation & management practices	Soil texture	Soil order	Parent material
Native prairies sites										
Derrhouse	Grand Island	40.73135	-98.56863	71	9-11	560-750	Prairies in this location support short, mid, and tall grasses, e.g., big bluestem, little bluestem, switchgrass, Indian grass, side oats grama, blue grama, western switchgrass, needle and thread, prairie sand reed, sand bluestem	Loamy Sand	Entisols and Mollisols	Loess
Pearl Harbor	Amherst	40.875022	-99.195397					Loam		
Marie Ratzlaff	Aurora	40.737911	-97.881464	75	10-12	590-800	Prairies in these locations support mid and tall grasses, e.g., big bluestem, little bluestem, switchgrass, Indian grass, side oats grama, western wheatgrass	Loam	Mollisols	Loess
Philips	Philips	40.919625	-98.207931					Sandy-loam		
Wildcat	Wachiska	40.16765	-96.526783					Sandy loam or sandy clay loam		

Belz	Norfolk	41.953158	-97.262828	102C	6.6-10.6	620-790	Prairie support little bluestem, big bluestem, switchgrass, western wheatgrass, Side oats grama, Porcupine, green needlegrass, and western wheatgrass	Loam or clay loam or silt loam	Mollisols	Loess
Nine-mile	Lincoln	40.86986	-96.80563	106	9.8-13.3	730-1040	Prairies in these locations support big bluestem, little bluestem, switchgrass, Indian grass, porcupine grass, side oats grama, switchgrass, and some wildrye	Loam	Mollisols, Alfisols, and Entisols	Loess
Pokorny	Midland	41.61277	-97.11305					Silt loam		
Prairie pine	Lincoln	40.844422	-96.567278					Loam		
Fricke	Fall city	40.151422	-95.539531					Loam or silt loam		
Zorinsky	Omaha	41.21543	-96.16649	107	6.7-13.4	700-1120	Prairies in this area support tall grasses and short grasses, e.g., blue grama, muhly, lovegrass, wheatgrass, little bluestem, big bluestem, Indian grass, and wild rye.	Silt loam	Mollisols and to a lesser degree Alfisol and Entisols	Loess
Arable sites										
Eddyville	Eddyville	41.014392	-98.624322	71	9-11	560-750	Corn, soybean, alfalfa, and seed crops were commonly grown in these areas.	Sandy clay loam or loam	Entisols and Mollisols	Loess

							Crops received water through precipitation (somewhat erratic) and irrigation (gravity and lateral-move pivot irrigation systems. Sites were under no-till, mulch-till and were fertilized. Cover crops commonly grown were cereal rye, ryegrass, hairy vetch, wheat, cowpea, and oat			
Pearl Harbor	Amherst	40.87485	-99.19735							
Knorr-Holden	Scottsbluff	41.944	-103.70041							
Wildcat	Wachiska	40.164144	-96.525508	75	10-12	590-800	Crops commonly grown were wheat and sorghum, but predominantly corn and soybean. Precipitation was moderate, somewhat erratic, and was the source of water for grain crops. In Clay Center and Philips, crops were irrigated using sub-surface drip and center pivot irrigation methods. Cover crops commonly grown were cereal rye,	Sandy loam or sandy clay loam	Mollisols	Loess

							ryegrass, hairy vetch, wheat, cowpea, radish, and mixed. Sites were under no-till and fertilized.			
Clay Center	Harvard	40.5743	-98.129056				.	Clay loam or loam		
Philips	Philips	40.922722	-98.215613					Sandy loam or sandy clay loam		
Dairyland	Firth	40.55361	-96.54539	106	10-13	730-1040	Crops grown were corn, soybean, and alfalfa. Precipitation is generally adequate for crop production in these areas except in Dairyland, where crops were irrigated (center-pivot irrigation) Cover crops commonly grown were cereal rye, ryegrass, hairy vetch, wheat, cowpea, radish, and mixed.	Loam	Mollisols, Alfisols, and Entisols	Loess
Pokorny	Midland	41.611606	-97.110539				sites were under no-till (except Rogers Memorial, under reduced tillage-chisel plow) and fertilized.	Silt loam		

Mead	Ithaca	40.85163	-96.46545					Silt loam or clay loam		
Rogers Memorial	Lincoln	40.85163	-96.46545					Silt loam or clay loam		
Glacier Creek	Omaha	41.3455	-96.1414	107B	6.7-13.4	700-1120	Major arable crops grown were corn and soybean. Precipitation is the main source of moisture for crops. Cover crops include ryegrass, hairy vetch, wheat, cowpea, radish, and cereal rye. The site was under no-till, mulch-till, and fertilized	Silt loam	Mollisols and, to a lesser degree, Alfisol and Entisols	Loess

ǂ USDA-NRCS (2022).
* For MAT and MAP, values are 30-year averages (1981-2010) based on the PRISM data set

Table S2. Range, mean, and standard error of soil available nitrate-N ($N\text{-}NO_3$), phosphate-P $P\text{-}PO_4$), and sulphate-S ($S\text{-}SO_4$) concentrations across arable and native prairie sites for A, B, and C horizons. Significant differences between land uses at $p \leq 0.05$ for each horizon are denoted by different letters.

Land use	Horizon	Depth ranges (cm) (upper and lower)	$N\text{-}NO_3$ (mg kg^{-1})	$P\text{-}PO_4$ (mg kg^{-1})	$S\text{-}SO_4$ (mg kg^{-1})
Arable	A	0-12-38	1.7-47 9 ± 1.9 a n=33	1.0-115 35 ± 5.6 a n=33	2.9-26 10 ± 0.8 a n=33
Native prairie	A	0-17-38	0.2-10 3 ± 0.4 b n=33	1.0-34 10 ± 1.5 b n=33	1.3-22 11 ± 0.7 a n=33
Arable	B	12-28-170	0.3-31 5 ± 1.0 cd n=40	1.0-81 15 ± 2.7 b n=40	1.3-55 13 ± 1.7 a n=40
Native Prairie	B	17-28-176	0.1-7.6 1.0 ± 0.2 e n=41	1.0-52 12 ± 1.8 b n=41	1.7-55 8.2 ± 1.3 a n=41
Arable	C	28-170-300	0.3-35 5 ± 0.9 d n=87	1.0-93 24 ± 2.6 c n=87	1.3-48 11 ± 1.0 a n=87
Native Prairie	C	28-176-300	0.2-8.8 0.9 ± 0.1 f n=80	1.0-57 16 ± 1.4 c n=80	1.2-53 9 ± 0.9 a n=80

n: total number of samples utilized for analysis from all A, B, and C horizons in arable and native prairie sites.

Table S3. Mean and standard error of soil organic carbon (SOC) stocks for individual arable (n=11) and native prairie (n=11) sites, showing the amount of SOC stored in 0-50, 50-100, 100-200, and 200-300 cm depth increments, as well as the cumulative value for the entire 0-300 cm depth. The mean values presented are site-specific and were derived from three replicated cores per site, with a total of 11 sites for each land use type.

Land use						
		SOC (kg m^{-2})				
Arable	Depth (cm)	0-50	50-100	100-200	200-300	0-300
Dairyland		10 ± 1.0	2.2 ± 0.3	4.0 ± 0.8	3.4 ± 0.3	19 ± 0.1
Pokorny		8.8 ± 1.1	7.8 ± 0.9	11 ± 1.8	6.8 ± 1.2	35 ± 0.1
Glacier creek		2.7 ± 0.1	1.9 ± 0.3	3.4 ± 0.4	3.5 ± 0.4	11 ± 0.1
Knorr-holden		2.7 ± 0.2	1.2 ± 0.5	1.1 ± 0.1	0.9 ± 0.1	5.9 ± 0.1
Roger's memorial		6.8 ± 1.3	4.0 ± 1.4	4.2 ± 1.4	3.0 ± 0.1	18 ± 0.3
Pearl harbor		5.7 ± 0.7	3.2 ± 0.7	3.3 ± 0.2	2.4 ± 0.1	14 ± 0.1
Wildcat		11 ± 1.9	4.0 ± 1.4	5.8 ± 1.0	4.2 ± 0.1	25 ± 0.3
Philips		8.7 ± 1.9	6.3 ± 2.3	6.8 ± 1.7	3.2 ± 0.3	25 ± 0.4

Mead		11 ± 0.1	9.5 ± 1.5	8.1 ± 1.8	5.1 ± 0.8	34 ± 0.3
Eddyville		3.9 ± 0.2	3.5 ± 0.3	6.5 ± 0.7	5.5 ± 0.5	19 ± 0.1
Clay center		5.2 ± 1.4	3.4 ± 2.0	3.0 ± 0.5	2.6 ± 0.2	14 ± 0.4
		SOC (kg m^{-2})				
Native prairie	Depth (cm)	0-50	50-100	100-200	200-300	0-300
Nine-mile		12 ± 0.9	4.8 ± 0.6	3.7 ± 0.5	2.8 ± 1.3	23 ± 0.2
Pokorny		17 ± 1.9	8.5 ± 1.7	5.7 ± 1.7	4.2 ± 1.0	35 ± 0.2
Zorinsky		7.8 ± 0.7	2.8 ± 0.4	4.7 ± 1.2	4.0 ± 0.6	19 ± 0.2
Derrhouse		4.0 ± 0.2	0.8 ± 0.2	0.6 ± 0.1	0.5 ± 0.02	6.0 ± 0.1
Prairie pine		9.7 ± 0.9	3.3 ± 0.5	4.5 ± 0.8	3.1 ± 0.2	20 ± 0.2
Pearl harbor		8.4 ± 2.6	5.3 ± 1.0	6.4 ± 0.3	3.4 ± 0.9	23 ± 0.4
Wildcat		9.7 ± 0.3	8.9 ± 1.0	8.9 ± 4.0	5.7 ± 3.9	33 ± 1.0

Philips		10 ± 1.2	4.1 ± 2.4	4.8 ± 1.6	3.3 ± 0.8	22 ± 0.3
Fricke		11 ± 0.9	3.4 ± 0.4	4.2 ± 1.0	2.4 ± 0.1	21 ± 0.2
Belz		10 ± 0.4	4.5 ± 0.3	7.6 ± 0.6	7.2 ± 0.8	29 ± 0.1
Marie Ratzlaff		8.6 ± 1.3	3.7 ± 1.9	3.6 ± 1.1	3.0 ± 0.9	19 ± 0.2

Table S4. Mean and standard error of soil total nitrogen (N_t) stocks for individual arable (n=11) and native prairie (n=11) sites, showing the amount of N_t stored in 0-50, 50-100, 100-200, and 200-300 cm depth increments, as well as the cumulative value for the entire 0-300 cm depth. The mean values presented are site-specific and were derived from three replicated cores per site, with a total of 11 sites for each land use type.

Land use						
		N_t (kg m^{-2})				
Arable	Depth (cm)	0-50	50-100	100-200	200-300	0-300
Dairyland		0.9 ± 0.1	0.3 ± 0.02	0.5 ± 0.1	0.5 ± 0.1	2.2 ± 0.01
Pokorny		0.6 ± 0.1	0.3 ± 0.02	0.6 ± 0.1	0.5 ± 0.1	1.9 ± 0.01
Glacier creek		0.3 ± 0.01	0.2 ± 0.03	0.4 ± 0.04	0.5 ± 0.03	1.4 ± 0.01
Knorr-holden		0.3 ± 0.02	0.2 ± 0.03	0.1 ± 0.01	0.09 ± 0.01	0.6 ± 0.004
Roger's memorial		0.6 ± 0.1	0.4 ± 0.1	0.5 ± 0.1	0.5 ± 0.01	2.1 ± 0.02
Pearl harbor		0.5 ± 0.1	0.3 ± 0.1	0.4 ± 0.01	0.5 ± 0.04	1.7 ± 0.01
Wildcat		0.9 ± 0.1	0.4 ± 0.1	0.7 ± 0.1	0.7 ± 0.1	2.8 ± 0.01
Philips		0.9 ± 0.1	0.7 ± 0.2	0.9 ± 0.1	0.6 ± 0.04	3.1 ± 0.03

Mead		0.8 ± 0.03	0.7 ± 0.1	0.6 ± 0.1	0.5 ± 0.1	2.6 ± 0.01
Eddyville		0.4 ± 0.01	0.2 ± 0.01	0.4 ± 0.04	0.4 ± 0.04	1.4 ± 0.01
Clay center		0.5 ± 0.1	0.4 ± 0.1	0.4 ± 0.04	0.5 ± 0.1	1.8 ± 0.02
		N_t (kg m^{-2})				
Native prairie	Depth (cm)	0-50	50-100	100-200	200-300	0-300
Nine-mile		0.9 ± 0.1	0.3 ± 0.1	0.3 ± 0.03	0.3 ± 0.01	2.0 ± 0.01
Pokorny		1.4 ± 0.1	0.7 ± 0.1	0.6 ± 0.1	0.6 ± 0.1	3.5 ± 0.01
Zorinsky		0.7 ± 0.1	0.2 ± 0.02	0.4 ± 0.04	0.4 ± 0.01	1.8 ± 0.01
Derrhouse		0.4 ± 0.02	0.15 ± 0.01	0.2 ± 0.1	0.2 ± 0.1	0.9 ± 0.01
Prairie pine		0.8 ± 0.1	0.3 ± 0.03	0.5 ± 0.1	0.4 ± 0.02	2.1 ± 0.01
Pearl harbor		0.6 ± 0.2	0.4 ± 0.1	0.5 ± 0.1	0.4 ± 0.01	2.0 ± 0.04
Wildcat		0.5 ± 0.1	0.2 ± 0.1	0.4 ± 0.1	0.4 ± 0.1	1.6 ± 0.004

Philips		1.2 ± 0.3	0.4 ± 0.1	0.5 ± 0.1	0.6 ± 0.1	2.9 ± 0.1
Fricke		0.9 ± 0.1	0.2 ± 0.03	0.4 ± 0.01	0.4 ± 0.1	1.9 ± 0.01
Belz		0.9 ± 0.04	0.4 ± 0.02	0.4 ± 0.02	0.4 ± 0.02	2.1 ± 0.004
Marie Ratzlaff		0.7 ± 0.1	0.4 ± 0.1	0.5 ± 0.1	0.4 ± 0.1	2.1 ± 0.02

Figure S5. Summary of the mean and standard error of soil organic carbon (SOC) and total nitrogen (N_t) stocks for the 11 arable and 11 native prairie sites, showing the amount of SOC and N_t stored in the 0-50 cm, 50-100 cm, 100-200 cm, and 200-300 cm depth increments, as well as the total amount in the 0-300 cm depth range.

Land use		**Depth (cm)**				
	SOC (Kg m^{-2})	0-50	50 -100	100 -200	200 -300	0 - 300
Arable sites (n=11)		7.0 ± 0.9	4.3 ± 0.7	5.3 ± 0.8	3.7 ± 0.4	20.3 ± 2.7
Native prairie sites (n=11)		9.9 ± 0.9	4.6 ± 0.7	5.0 ± 0.6	3.6 ± 0.5	23.2 ± 2.4
	STN (Kg m^{-2})	0-50	50 -100	100 -200	200 -300	0 - 300
Arable sites (n=11)		0.6 ± 0.1	0.4 ± 0.1	0.5 ± 0.1	0.5 ± 0.1	2.0 ± 0.2
Native prairie sites (n=11)		0.9 ± 0.1	0.4 ± 0.1	0.5 ± 0.1	0.4 ± 0.1	2.2 ± 0.2

Table S6. Summary of range, mean, standard error, and sample size (n) (number of measurements per horizon and land use type) for $\Delta^{14}C$ of bulk soil organic carbon across, showing the radiocarbon ages across A, B, and C horizons in arable and native prairie soils. BP signifies "before present."

Land use				
		$\Delta^{14}C$ (‰) (^{14}C age in years BP)		
	Horizons	A	B	C
Arable		(1102 ± 240 yrs.) n= 9	(6415 ± 1502 yrs.) n=6	(11933 ± 920 yrs.) n=18
Native prairie		(190 ± 48 yrs.) n=10	(5161 ± 1224 yrs.) n=6	(11930 ± 1046 yrs.) n=22